Development of potent and selective FAAH inhibitors with improved drug-like properties as potential tools to treat neuroinflammatory conditions

European Journal of Medicinal Chemistry

Development of potent and selective FAAH inhibitors with improved drug-like properties as potential tools to treat neuroinflammatory conditions

--Manuscript Draft--

Manuscript Number:	EJMECH-D-22-02439R1
Article Type:	Full Paper
Keywords:	Endocannabinoid system; Fatty acid amide hydrolase; Enzyme inhibitors; Selective inhibitors; Neuroinflammation; Neuroprotection, Reversible inhibitors
Corresponding Author:	Stefania Butini, Ph.D. University of Siena: Universita degli Studi di Siena siena, ITALY
First Author:	Alessandro Papa
Order of Authors:	Alessandro Papa
	Silvia Pasquini
	Francesca Galvani
	Mariarosaria Cammarota
	Chiara Contri
	Gabriele Carullo
	Sandra Gemma
	Anna Ramunno
	Stefania Lamponi
	Beatrice Gorelli
	Simona Saponara
	Katia Varani
	Marco Mor
	Giuseppe Campiani
	Francesca Boscia
	Fabrizio Vincenzi
	Alessio Lodola
	stefania butini
Abstract:	The neuroprotective performance against neuroinflammation of the endocannabinoid system (ECS) can be remarkably improved by indirect stimulation mediated by the pharmacological inhibition of the key ECS catabolic enzyme fatty acid amide hydrolase (FAAH). Based on our previous works and aiming to discover new selective FAAH inhibitors (4a-t), we herein reported a new series of carbamate-based FAAH inhibitors which showed improved drug disposition properties compared to the previously reported analogues 2a-b. The introduction of ionizable functions allowed us to obtain new FAAH inhibitors of nanomolar potency characterized by good water solubility and chemical stability at physiological pH. Interesting structure-activity relationships (SARs), deeply analyzed by molecular docking and dynamic simulations, were obtained. All the newly developed inhibitors showed an excellent selectivity profile evaluated against monoacylglycerol lipase and cannabinoid receptors. The reversible mechanism of action was determined by a rapid dilution assay. Absence of toxicity was confirmed in mouse fibroblasts NIH3T3 (for compounds 4e, 4g, 4n-o, and 4s) and in human astrocytes cell line 1321N1 (for compounds 4e, 4n, and 4s). The absence of undesired cardiac effects was also confirmed for compound 4n. Selected analogues (compounds 4e, 4g, 4n, and 4s) were able to reduce oxidative stress in 1321N1

	astrocytes and exhibited notable neuroprotective effects when tested in an ex vivo model of neuroinflammation.
Suggested Reviewers:	Mario van der Stelt m.van.der.stelt@chem.leidenuniv.nl
	Vinod Kumar vpathania18@gmail.com
	Antti Poso antti.poso@uef.fi
	Holger Stark stark@hhu.de
	José Marco-Contelles jlmarco@iqog.csic.es
	Andrea Cavalli andrea.cavalli@iit.it

Development of potent and selective FAAH inhibitors with improved drug-like properties as potential tools to treat neuroinflammatory conditions

Alessandro Papa,[a] Silvia Pasquini,[b] Francesca Galvani,[c] Mariarosaria Cammarota,[d] Chiara Contri,[e] Gabriele Carullo,[f] Sandra Gemma,[a] Anna Ramunno,[g] Stefania Lamponi,[a] Beatrice Gorelli,[f] Simona Saponara,[f] Katia Varani,[e] Marco Mor,[c,h] Giuseppe Campiani,[a] Francesca Boscia,[d,◊] Fabrizio Vincenzi,[e,◊] Alessio Lodola,[c,◊] Stefania Butini,[a,◊,*]

[a]Dipartimento di Biotecnologie, Chimica e Farmacia, Università degli Studi di Siena, Via Aldo Moro 2, 53100, Siena, Italy
[b]Dipartimento di Scienze Chimiche, Farmaceutiche e Agrarie, Università degli Studi di Ferrara, Via Borsari 46, 44121, Ferrara, Italy
[c]Dipartimento di Scienze degli Alimenti e del Farmaco, Università degli Studi di Parma, Parco Area delle Scienze 27/A, 43124 Parma, Italy
[d]Divisione di Farmacologia, Dipartimento di Neuroscienze e Scienze Riproduttive ed Odontostomatologiche, Università degli Studi di Napoli Federico II, Via Pansini 5, 80131 Napoli, Italy
[e]Dipartimento di Medicina Traslazionale e per la Romagna, Università degli Studi di Ferrara, Via Borsari 46, 44121, Ferrara, Italy
[f]Dipartiment di Scienze della Vita, Università degli Studi di Siena, Via Aldo Moro 2, 53100, Siena, Italy
[g]Dipartimento di Farmacia, Università degli Studi di Salerno, Viale Giovanni Paolo II 132, 84084, Fisciano (SA), Italy
[h]Microbiome Research Hub, Università degli Studi di Parma, Parco Area delle Scienze 11/A, I-43124 Parma, Italy

[◊]Co-last authors

Author for correspondence: Stefania Butini e-mail butini3@unisi.it

Abstract

The neuroprotective performance against neuroinflammation of the endocannabinoid system (ECS) can be remarkably improved by indirect stimulation mediated by the pharmacological inhibition of the key ECS catabolic enzyme fatty acid amide hydrolase (FAAH). Based on our previous works and aiming to discover new selective FAAH inhibitors (**4a-t**), we herein reported a new series of carbamate-based FAAH inhibitors which showed improved drug disposition properties compared to the previously reported analogues **2a-b**. The introduction of ionizable functions allowed us to obtain new FAAH inhibitors of nanomolar potency characterized by good water solubility and chemical stability at physiological pH. Interesting structure-activity relationships (SARs), deeply analyzed by molecular docking and dynamic simulations, were obtained. All the newly developed inhibitors showed an excellent selectivity profile evaluated against monoacylglycerol lipase and cannabinoid receptors. The reversible mechanism of action was determined by a rapid dilution assay. Absence of toxicity was confirmed in mouse fibroblasts NIH3T3 (for compounds **4e**, **4g**, **4n-o**, and **4s**) and in human astrocytes cell line 1321N1 (for compounds **4e**, **4n**, and **4s**). The absence of undesired cardiac effects was also confirmed for compound **4n**. Selected analogues (compounds **4e**, **4g**, **4n**, and **4s**) were able to reduce oxidative stress in 1321N1 astrocytes and exhibited notable neuroprotective effects when tested in an *ex vivo* model of neuroinflammation.

Keywords

Endocannabinoid system; Fatty acid amide hydrolase; Enzyme inhibitors; Selective inhibitors; Neuroinflammation; Neuroprotection, Reversible inhibitors.

Abbreviations

2-AG: 2-arachidonoylglycerol, AD: Alzheimer's disease, AEA: anandamide, ALS: amyotrophic lateral sclerosis, CBR_1: cannabinoid receptor type 1, CBR_2: cannabinoid receptor type 2, CNS: central nervous system, DCM: dichloromethane, DMF: dimethylformamide, eCBs: endocannabinoids, ECS: endocannabinoid system, EtOH: ethanol, FAAH: fatty acid amide hydrolase, HR: frequency, IFN-γ: interferon-γ, IL-10: Interleukin-10, IL-1β: Interleukin-1β, LPS: lipopolysaccharide, MAGL: monoacylglycerol lipase, MeOH: methanol, MS: multiple sclerosis, NAC: N-acetylcysteine, OS: oxidative stress, PD: Parkinson's disease, PI: propidium iodide, PQ: atrioventricular conduction time, QRS: intraventricular conduction time, QT: action potential duration, ROS: reactive oxygen species, RR: cycle length, SAR: structure activity relationship, TBHP: *tert*-butyl hydroperoxide, TCICA: trichloroisocyanuric acid, TEA: triethylamine, TEMPO: (2,2,6,6-tetramethylpiperidin-1-yl)oxidanyl, TFA: trifluoroacetic acid, THF: tetrahydrofuran, TNF-α: tumor necrosis factor-α.

1. Introduction

Endocannabinoids (eCBs) are a class of lipid mediators synthesized on demand, including amides or esters of long-chain polyunsaturated fatty acids [1]. Among these, anandamide (AEA) and 2-arachidonoylglycerol (2-AG) exert major pro-homeostatic functions through the activation of cannabinoid type 1 and type 2 receptors (CBR_1 and CBR_2) [1–3]. Analogously to other lipid mediators, the eCBs are rapidly inactivated by a two-step process involving carrier-mediated uptake followed by enzymatic degradation. Enzymatic catabolism is primarily operated by fatty acid amide hydrolase (FAAH) and monoacylglycerol lipase (MAGL), which catabolize AEA and 2-AG respectively [1,4]. FAAH is an integral membrane enzyme belonging to the serine hydrolase superfamily. The 3D structure of FAAH reveals its homodimeric nature, characterized by an atypical Ser241-Ser-217-Lys142 catalytic triad [5–7]. Inactivation of FAAH elevates endogenous levels of AEA, promoting the beneficial effects of endocannabinoid system (ECS) stimulation in several pathophysiological processes such as excitotoxicity conditions, neurodegeneration, oxidative stress (OS) and neuroinflammation [8–10]. Neurological disorders can be triggered by chronic neuroinflammatory conditions that, through different mechanisms in which the OS is involved, may lead to neuronal cell death [11,12]. OS is caused by increased levels of reactive oxygen species (ROS) deriving from mitochondrial dysfunctions [13]. Neuroinflammation, mainly orchestrated by glial cells, is a common feature of several neurodegenerative and demyelinating diseases, such as Alzheimer's disease (AD), Parkinson's disease (PD), amyotrophic lateral sclerosis (ALS) and multiple sclerosis (MS) [12,14,15]. In microglia and astrocytes, AEA attenuates the release of pro-inflammatory mediators, such as tumor necrosis factor-α (TNF-α), IL-1β and nitric oxide, and increases the levels of the anti-inflammatory cytokine IL-10 [16]. Accordingly, URB-597 (**1**, Figure 1), one of the most investigated carbamate-based FAAH inhibitors, shows anti-inflammatory effects, due to decreased levels of pro-inflammatory cytokines such as IL-1β and TNF-α, when administered in aged rats [17]. These data suggest the relevant role of FAAH and AEA in the regulation of neuro-inflammatory states.

One of the aims of our research activity is focused on the exploitation of the catabolism of AEA to generate evidence-based novel therapeutics [18–20]. In this context, we recently disclosed potent and selective FAAH inhibitors typified by compounds **2a,b** (Figure 1), which were moved towards an unconventional application in the context of epilepsy [21]. As a further aim, we recently embarked in a polypharmacological approach where FAAH inhibition was combined to dopamine receptor antagonism [22]. To this end, we anchored over the arylfurane-based scaffolds of our FAAH inhibitors a polar phenylpiperazine lateral chain (as in compound **3**, Figure 1). This moiety improved key physico-chemical properties including hydrophilic/lipophilic balance, water solubility and chemical stability, known to affect carbamate disposition in biological assays [23].

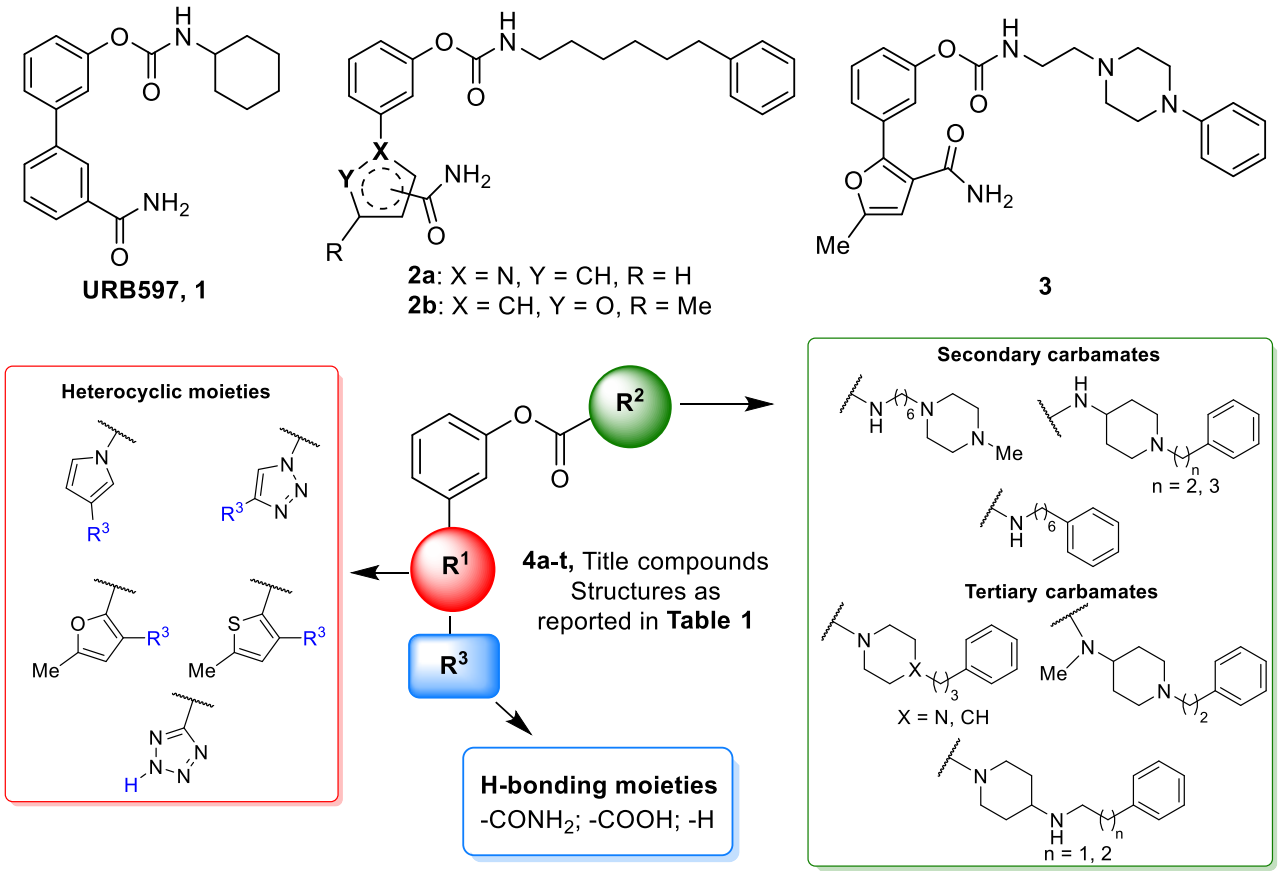

Figure 1. Reference (**1-3**) and title compounds (**4a-t**).

In the search for potent and selective FAAH inhibitors with improved physico-chemical properties, we designed novel classes of *O*-arylcarbamates in which basic and/or acidic fragments were

inserted in the structure of our reference inhibitors **2a** and **2b**. The effect of tertiarization of the carbamate nitrogen was also explored to reduce the reactivity of the compounds in acidic and neutral media. This set of modifications led to the synthesis of compounds **4a-t** which were evaluated for FAAH inhibitory potency, FAAH/MAGL selectivity, solubility, and chemical stability. For a selected subset of analogues, the selectivity profile towards cannabinoid CBR_1 and CBR_2 was further investigated. For selected analogues, cytotoxicity was evaluated in murine fibroblasts and in 1321N1 astrocytes. The most promising compounds **4e**, **4n** and **4s** effectively reduced ROS production in 1321N1 astrocytes. Absence of cardiac side-effects was also evaluated for compound **4n**. Finally, we assessed the neuroprotective effects of compounds **4e**, **4g**, **4n** and **4s** against inflammation-induced neurodegeneration in *ex vivo* cultures of rat hippocampal explants.

2. Results and discussion

2.1. Chemistry

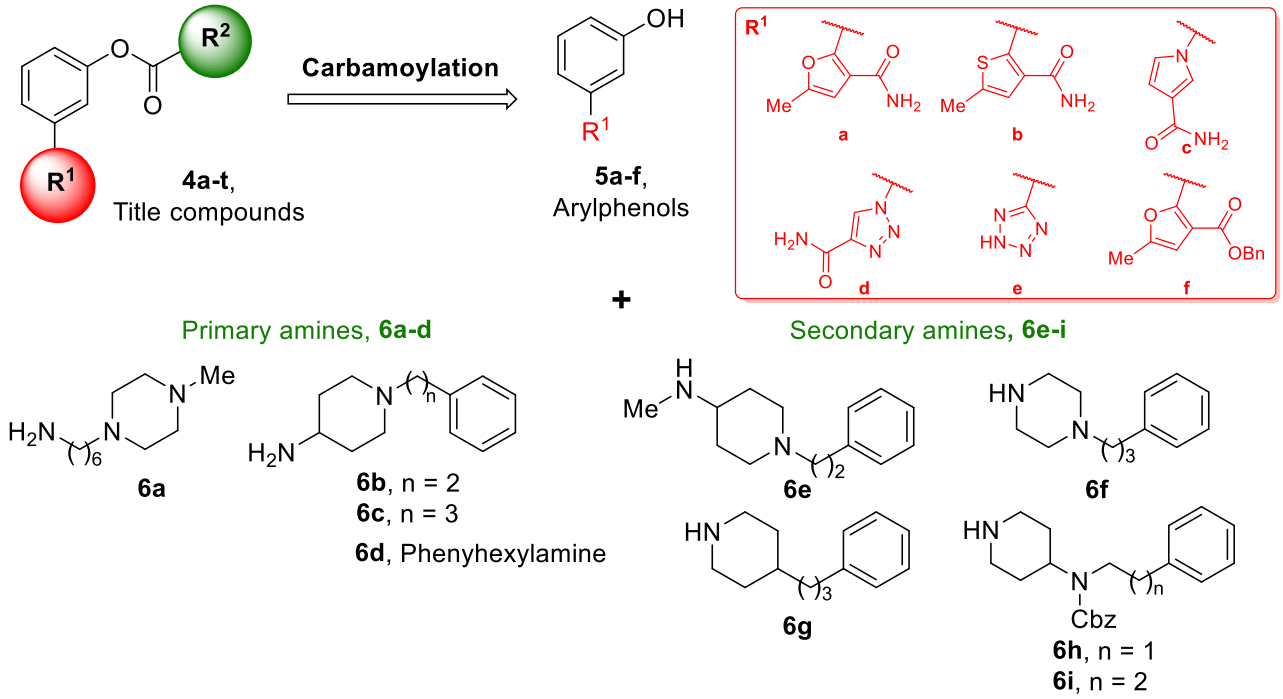

Figure 2. Retrosynthetic analysis.

The synthesis of compounds **4a-t** is reported in the Schemes 1-5. According to our retrosynthetic analysis (Figure 2), all the compounds were obtained by using a convergent approach. The bisaryl phenols **5a-f** could be reacted with a multitude of primary (**6a-d**) or secondary amines (**6e-i**) in the

presence of *p*-nitrophenyl chloroformate to generate the final compounds (**4a-f, 4i-p** and **4s-t**) or their appropriately protected analogues. The required non-commercially available amines (**6a-c,e-i**) could be synthesized by applying reductive amination protocols engaging the appropriate amine and the corresponding aldehydes or *N*-alkylation of the appropriate amines. Upon the need of different functional groups, an orthogonal protection strategy was applied to obtain selective and effective deprotection in the different stages of the synthetic process as detailed in the Schemes 2-4.

The synthesis of phenols **5e**,**f** is depicted in Scheme 1. **5e** was obtained by a cycloaddition reaction involving the 3-cyanophenol **7** and sodium azide in the presence of triethylammonium chloride. For compound **5f**, the methoxy functionality of compound **8** [18] was cleaved using boron tribromide to give the phenol intermediate **9** that was protected as benzyl ester.

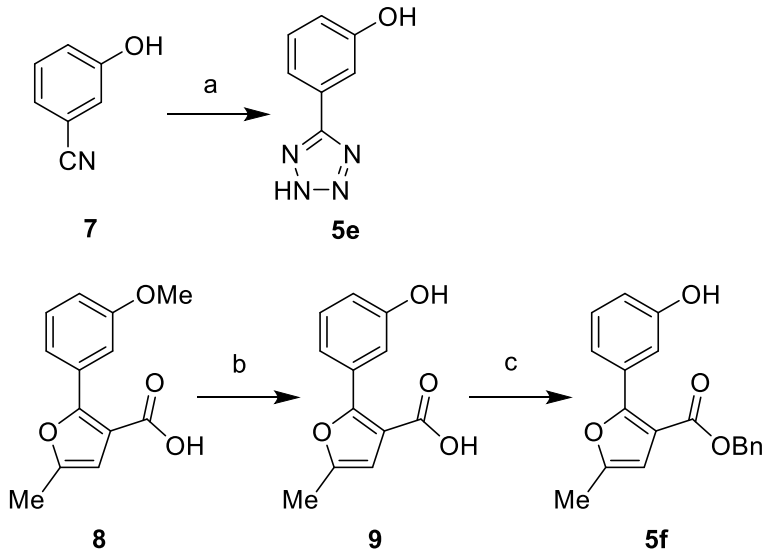

Scheme 1. Synthesis of phenols **5e** and **5f**.
Reagents and conditions. a) triethylamine (TEA) hydrochloride, sodium azide, dry toluene, 110 °C, 20 h, 45%; b) BBr_3, dry DCM, from -78 °C to 25 °C, 2 h, 99%; c) benzyl bromide, $NaHCO_3$, dry DMF, 40 °C, 12 h, 70%.

The synthesis of the primary amines **6a-c** is reported in Scheme 2. Alkylation of 1-methylpiperazine **10** using 5-bromovaleronitrile gave intermediate **11** which was reduced by $LiAlH_4$ leading to amine **6a**. Alkylation of 4-*N*-Boc-aminopiperidine **12** with 2-(bromoethyl)benzene gave the derivative **13**, which was then deprotected in presence of TFA to obtain the amine **6b**. To obtain the amine **6c**, 4-amino-*N*-Boc-piperidine **14** was previously protected as benzyl carbamate **15** and then subjected to

a selective Boc deprotection, furnishing **16**. This latter was treated with aldehyde **18** to furnish *N*-alkyl derivative **19** that generated the amine **6c** after Cbz removal. The synthesis of the needed aldehyde **18** started from 3-phenylpropanol **17** which underwent a (2,2,6,6-tetramethylpiperidin-1-yl)oxidanyl (TEMPO)-catalyzed oxidation that employs trichloroisocyanuric acid (TCICA) [24] to obtain the aldehyde in a quantitative yield.

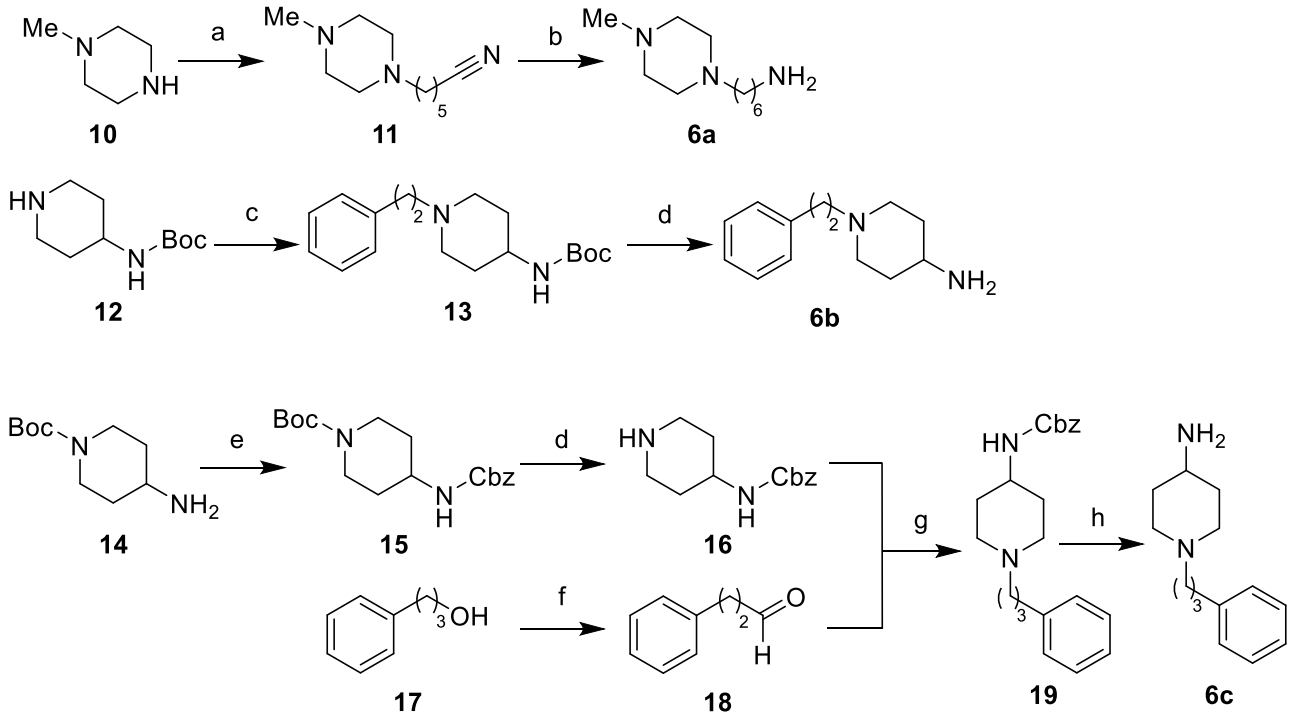

Scheme 2. Synthesis of primary amines **6a-c**.
Reagents and conditions. a) 5-bromovaleronitrile, Na_2CO_3, EtOH, 25 °C, 12 h, 25%; b) $LiAlH_4$, dry THF, 0 °C to 25 °C 1 h, 95%; c) 2-bromo ethylbenzene, TEA, dry THF, 70 °C, 12 h, 88%; d) TFA, dry DCM, from 0 °C to 25 °C 2 h, 95-99%; e) benzyl chloroformate, $NaHCO_3$, THF, 0 °C to 25 °C, 12 h, 80%; f) TEMPO, TCICA, dry DCM, 0 °C, 15 min, 99%; g) $NaBH(OAc)_3$, dry DCM, 25 °C, 12 h, 66%; h) H_2, Pd/C, MeOH, 25 °C, 2 h, 75%.

Secondary amines **6e-g** were synthesized according to Scheme 3. The treatment of compound **13** with $LiAlH_4$ furnished the *N*-methyl derivative **6e**. The 1-(3-phenylpropyl)piperazine **6f** was obtained by a conversion of the commercially available 3-phenylpropan-1ol **17** to the corresponding bromoderivative **20**. The nucleophilic substitution of 1-Boc-piperazine with **20** gave compound **21**, which was then subjected to a Boc deprotection. The application of the Wittig protocol between the triphenyl(3-phenylpropyl)phosphonium bromide **24**, in turn obtained from the

bromoderivative **20**, and benzyl piperidone **23**, in turn obtained from *N*-alkylation of **22**, led to the unsaturated product **25**. Catalytic hydrogenation of the olefin **25** furnished the amine **6g**.

For the orthogonally Cbz-protected secondary amines **6h,i**, we applied the synthesis reported in Scheme 4. Under reductive amination conditions, the phenylethylamine, *N*-Boc-piperidone **26** and $NaBH(OAc)_3$ provided compound **27** which was then treated with benzyl chloroformate to obtain derivative **28**. Orthogonal deprotection of the Boc group under acidic conditions led to amine **6h**. To obtain **6i**, 4-amino-*N*-Boc-piperidine **14** was subjected to a reductive amination protocol in the presence of the aldehyde **18** affording the derivative **29**. Introduction of the Cbz protecting group gave the intermediate **30,** which after Boc deprotection provided the desired amine **6i**.

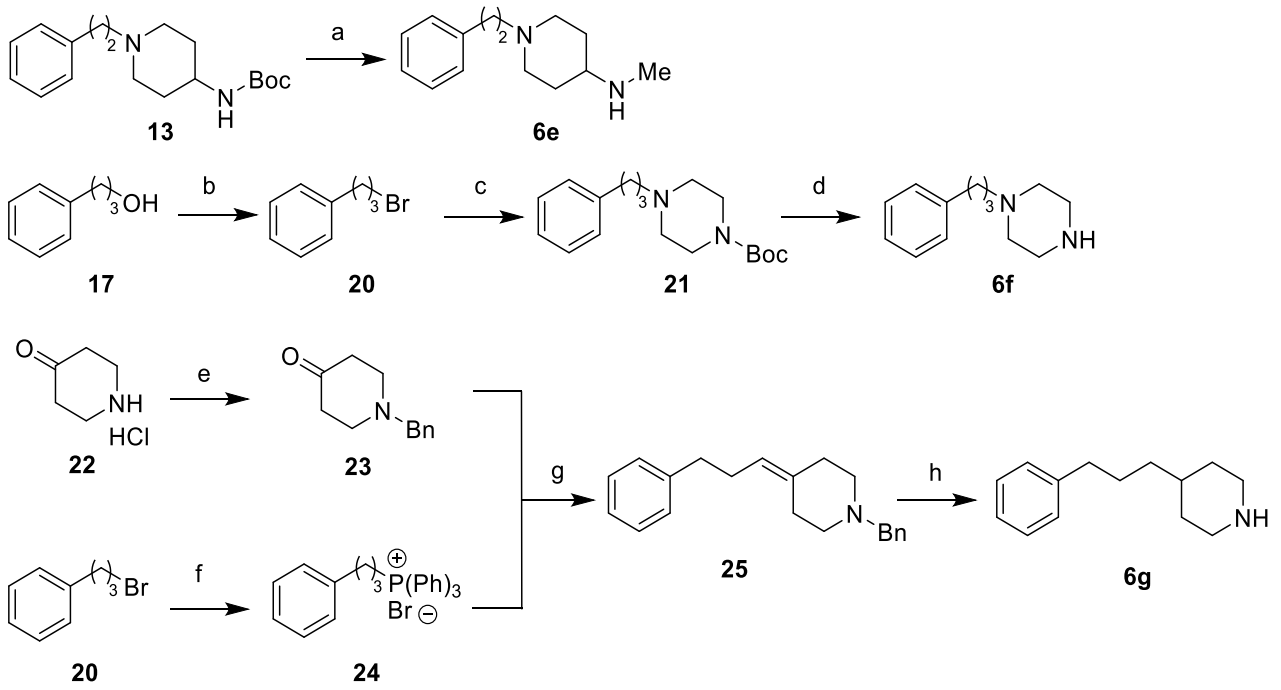

Scheme 3. Synthesis of secondary amines **6e-g**.
Reagents and conditions: a) $LiAlH_4$, dry THF, 0 °C to 70 °C 18 h, 63%; b) PPh_3, CBr_4, 1*H*-imidazole, dry DCM, 25 °C, 12 h, 95%; c) *N*-Boc-piperazine, K_2CO_3, KI, dry acetonitrile, 25 °C, 12 h, 93%; d) TFA, dry DCM, from 0 °C to 25 °C, 2 h, 99%; e) benzyl bromide, K_2CO_3, dry DMF, 75 °C, 12 h, 70%; f) PPh_3, dry toluene, 110 °C, 24 h, 26%; g) *n*-butyllithium (1.6 M in hexane), dry THF, from 0 °C to 25 °C, 12 h, 28%; h) Pd/C, H_2, MeOH, 25 °C, 2 h, 82%.

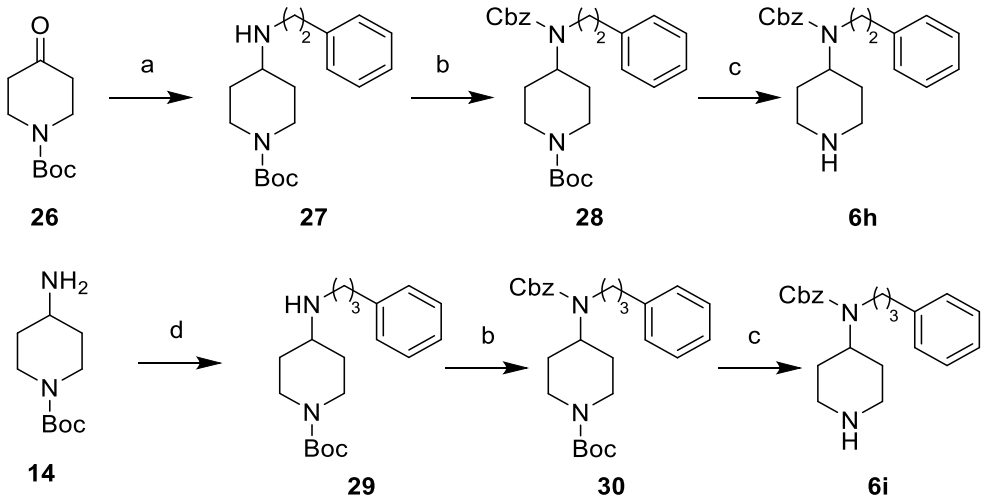

Scheme 4. Synthesis of secondary amines **6h,i**.
Reagents and conditions: a) $NaBH(OAc)_3$, phenylethylamine, dry DCM, 25 °C, 12 h, 62%; b) benzyl chloroformate, $NaHCO_3$, THF, from 0 °C to 25 °C, 12 h, 99-88%; c) TFA, dry DCM, 0 °C to 25 °C 2 h, 87-99%%; d) $NaBH(OAc)_3$, aldehyde **18**, dry DCM, 25 °C, 12 h, 60%.

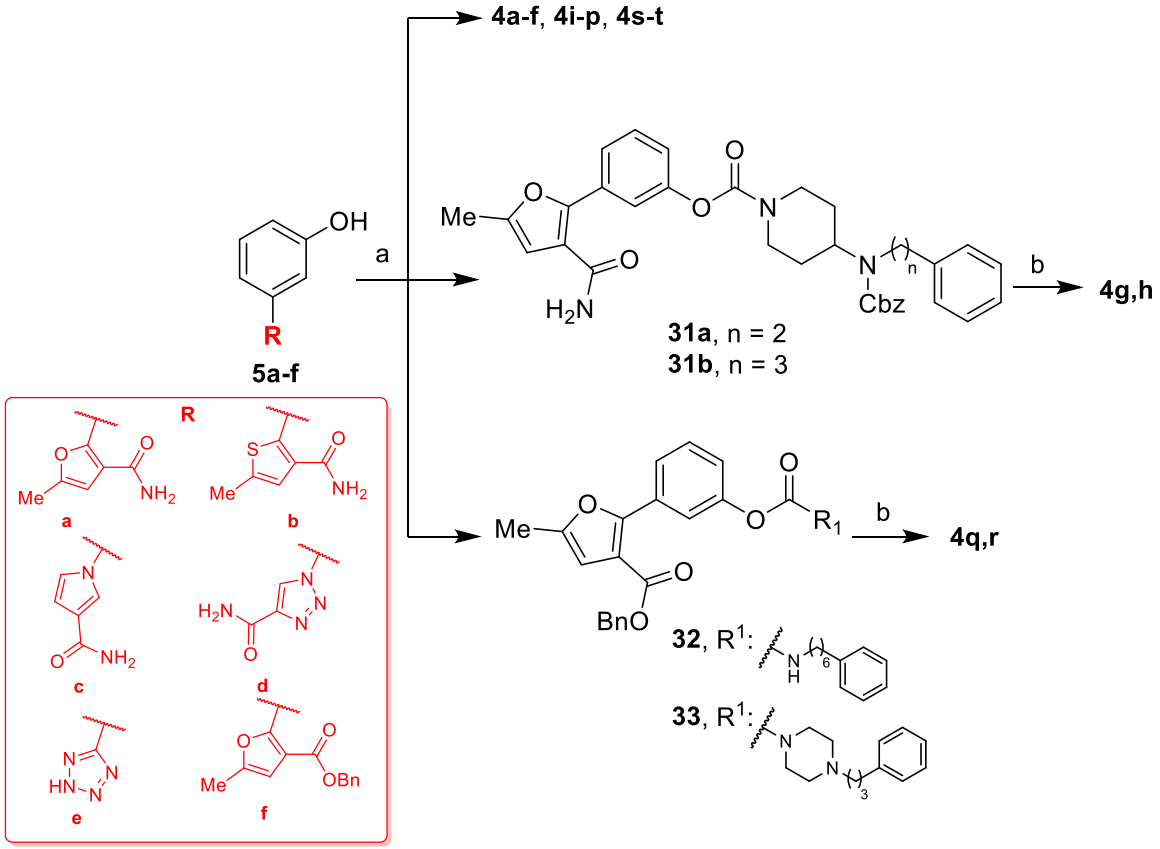

Scheme 5. Synthesis of compounds **4a-t**.
Reagents and conditions: a) 4-nitrophenyl chloroformate, TEA, dry DCM, 0 °C to 25 °C, 4 h, and suitable amine, 17-64%; b) H_2, Pd/C, MeOH/EtOAc, 25 °C, 2 h, 13-74%.

The final steps for the synthesis of compounds **4a-t** are depicted in Scheme 5. The phenols **5a-c** [18], **5d** [22] and the newly developed phenol derivatives **5e,f** (Scheme 1) were combined with the

corresponding amines to form secondary or tertiary carbamates in the presence of 4-nitrophenyl chloroformate (Scheme 5). By choosing the appropriate combination of phenol derivative and amine the final compounds were obtained. Briefly, the phenol **5a** was combined with amines **6a-c** and **6e-g** to obtain carbamates **4a-c** and **4d-f** respectively. **5a** was also reacted with amines **6h,i** to obtain the protected intermediates **31a** and **31b**. From these latter, Cbz deprotection provided the target compounds **4g-h**. Phenols **5b-c** were combined with amines **6b**, **6e** and **6f** to obtain compounds **4i-k** and **4l-n** respectively. Phenols **5d-e** were combined with phenylhexyl amine **6d** [18] and amine **6f** to obtain derivatives **4o-p** and **4s-t** respectively. Phenol **5f** was combined with phenylhexyl amine **6d** [18] and amine **6f** to obtain the intermediates **32** and **33** that gave **4q-r** following a palladium catalyzed hydrogenation to remove the benzyl group.

Table 1. Inhibitory activity towards *human* FAAH and *human* MAGL (expressed as IC_{50} nM) for title compounds **4a**–**t**, and reference compounds **2a**-**b**.

Cmpds	Structure	IC_{50} (nM) *h*FAAH[a]	IC_{50} (nM) *h*MAGL[a]
4a	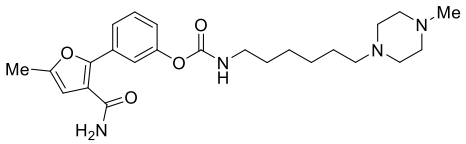	1044 ± 73	>10000
4b	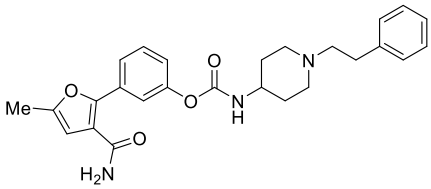	188 ± 11	>10000
4c	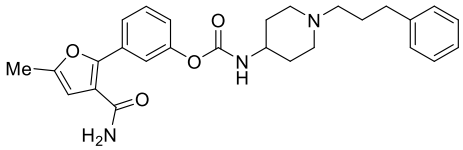	407 ± 32	>10000
4d	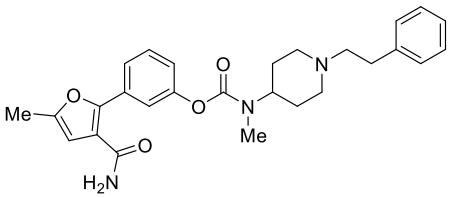	6556 ± 412	>10000
4e	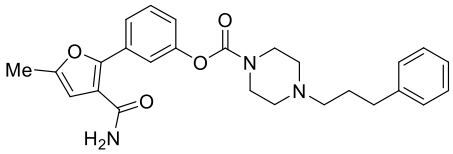	8.29 ± 0.58	5061 ± 387
4f	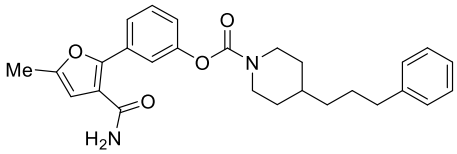	11.7 ± 0.8	4116 ± 314
4g	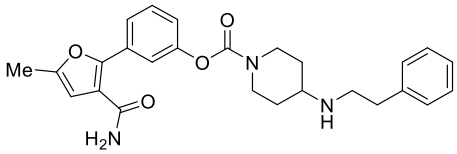	26.3 ± 2.1	>10000
4h	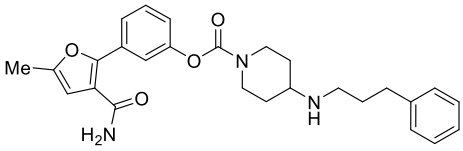	165 ± 12	9878 ± 677
4i	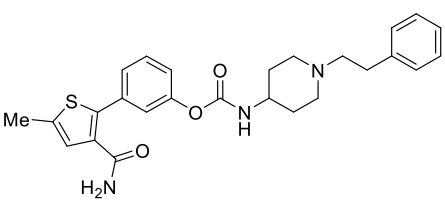	194 ± 13	>10000

4j	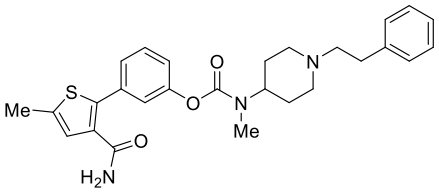	8450 ± 523	>10000
4k	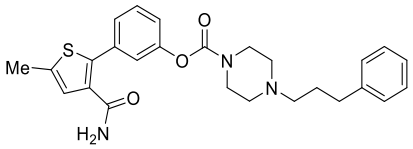	15.6 ± 0.9	>10000
4l	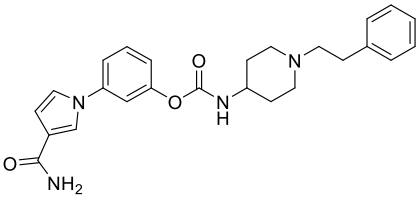	315 ± 19	>10000
4m	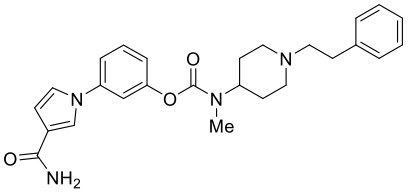	>10000	>10000
4n	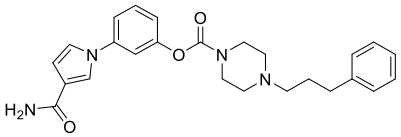	10.1 ± 0.6	>10000
4o	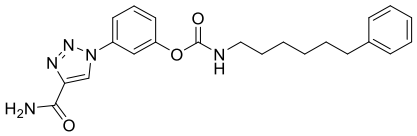	15.8 ± 1.1	479 ± 28
4p	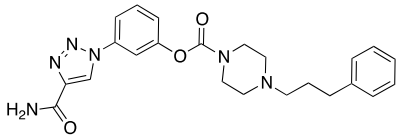	47.4 ± 2.8	2899 ± 193
4q	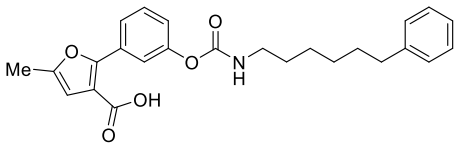	10.5 ± 0.8	2437 ± 178
4r	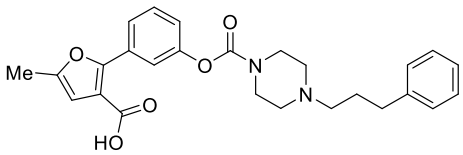	128 ± 9	>10000
4s	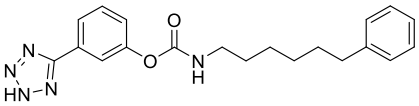	7.54 ± 0.51	8396 ± 621
4t	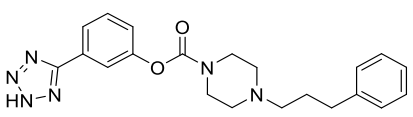	253 ± 13	>10000
2a	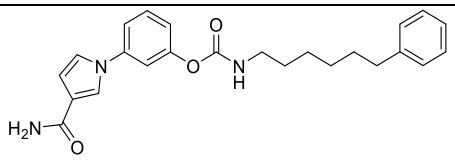	3.72 ± 0.21	-[18]

2b	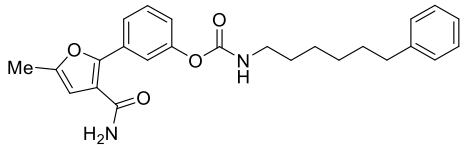	102 ± 9 [18]	-[18]
1	-	31.1 ± 1.8	9384 ± 652

[a]Each value represents the mean ± SEM of three independent experiments. Differences were considered statistically significant at * $p < 0.05$. FAAH and MAGL inhibition was measured after 30 min of pre-incubation; [b]NT not tested; [c]NC not calculable.

2.2. Structure activity relationship studies and molecular modelling studies

FAAH activity was measured on a *human* recombinant purified enzyme following a 30 min pre-incubation with the tested compounds. Half-maximal inhibitory concentration (IC_{50}) values for compounds **4a**-**t** are reported in Table 1, along with that of the reference phenylpyrrole **2a** and phenylfurane **2b**. The goal of our investigation was the identification of compounds with balanced potency on FAAH, solubility, chemical stability and lack of activity on MAGL (*vide infra*). Given the poor water solubility of compounds **2a**-**b** in order to improve this physico-chemical property while preserving inhibitory potency on FAAH, we firstly assessed the tolerance of FAAH towards the introduction of a basic center in the bulky substituent at the nitrogen atom and/or the tertiarization of carbamate group. Substitution of the terminal phenyl substituent of arylfuran **2b** with a 4-methylpiperazine group (compound **4a**) resulted in a 10-fold decrease in the inhibitory potency. The loss in activity was less prominent when a 4-phenylalkylpiperidine was introduced at the nitrogen atom as in the case of **4b** and **4c**, displaying IC_{50} values of 188 and 407 nM, respectively. Tertiarization of the carbamate group of **4b** had a different impact on inhibitory potency, with direct methylation of the nitrogen dramatically reducing activity (**4d**, IC_{50} = 6556 nM), and its inclusion in a piperazine ring leading to a single digit nanomolar compound (**4e**, IC_{50} = 8.3 nM). Compound **4e** thus emerged as key inhibitor deserving further investigations, considering our multiparametric optimization aimed at finding inhibitors with good potency and balanced physico-chemical properties. Replacement of the 4-(3-phenylpropyl)piperazine of **4e** with a 4-(3-

phenylpropyl)piperidine substituent, avoiding a basic center, was well tolerated by FAAH with **4f** having an IC_{50} value (11.7 nM) approaching that of **4e**. A loss in the inhibitory potency was observed when the 4-(3-phenylpropyl)piperazine moiety of **4e** was replaced by, likely more basic, 4-(phenylalkylamino)piperidine chains of **4g** and **4h**, displaying IC_{50} values of 26 and 165 nM, respectively. This trend suggests that FAAH preferentially recognizes the neutral form of tested inhibitors, and that an increment in the pK_a of the substituent incorporating the nitrogen atom of the carbamate hampers inhibitory potency by reducing the availability of the neutral species.

To corroborate this hypothesis, a computational analysis was performed. Docking and molecular dynamics (MD) simulations were performed to evaluate the preference displayed by FAAH active site for the neutral or the protonated form of compound **4e**, while a density functional theory (DFT) approach was applied to estimate pK_a constant values of **4e** and **4g**.

When docked in FAAH with Glide software [25], both the neutral and protonated forms of compound **4e** assumed, as a best pose, a binding mode consistent with the X-ray structure of FAAH-URB597 covalent adduct [26] i.e. with the electrophilic carbon of the carbamate placed at nearly 3.0 Å from Ser241 hydroxyl oxygen, a distance consistent with a nucleophilic attack [27], the 3-(3-carbamoyl-5-methylfuran-2-yl)phenoxy group harbored in the solvent exposed cytoplasmic access (CA) channel, and the 4-(3-phenylpropyl)piperazine moiety accommodated in the acylchain-binding (ACB) pocket. Visual inspection of the FAAH-**4e** docking models (Figure 3) showed that while the terminal 3-$CONH_2$ substituent emerging from the furan ring formed H-bonds with CA channel residues (Cys269, Val270 NH groups), the phenylpropylpiperazine fragment did not undertake any polar interaction with the ACB pocket, being this region mostly composed by hydrophobic residues, including Phe192, Tyr194, Leu380, Phe381, Phe432 and Val491.

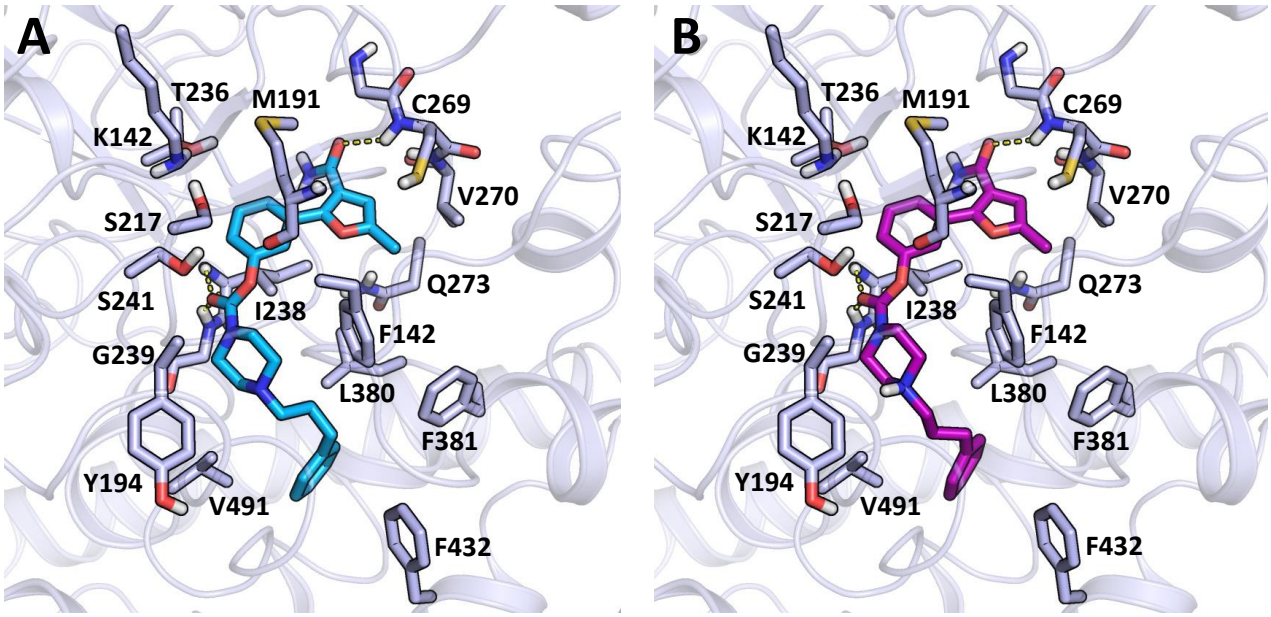

Figure 3. Best pose for compound **4e** docked into FAAH (light violet carbon atoms) in neutral (cyan carbon atoms, panel A) or protonated form (purple carbon atoms, panel B). The residues of the catalytic Lys142-Ser217-Ser241 triad are also displayed. In evidence the tertiary carbamate of **4e** accommodated in oxyanion hole and well oriented to react with Ser241 nucleophile.

The 100 ns-long MD simulations performed with Desmond/OPLS4 engine [28] showed that **4e** maintained an arrangement consistent with the docked pose only when modelled in the neutral form. The presence of a protonated piperazine in the ACB pocket increased the mobility of **4e** already in the early phases of MD simulations, pushing the carbamate group away from both the oxyanion hole and the nucleophile, stabilizing a disposition not compatible with Ser241 carbamoylation (Figure S1, of the Supplementary Information). MD simulations replicates gave similar results (Figure S2).

A hybrid computational approach available in Jaguar software [29], coupling DFT calculations with an empirical correction based on high-quality experimental data [30], was applied to estimate the pK_a constant values of compounds **4e** and **4g** (see Experimental section for details). This approach predicted a higher pK_a value for 4-(phenylethylamino)piperidine **4g** than for 4-(3-phenylpropyl)piperazine **4e**, with computed values of 8.5 and 7.6, respectively. This suggests that for compound **4g** a lower fraction of the neutral form is available for FAAH binding, qualitatively

accounting for its lower potency displayed in the wet assay (IC_{50} = 26 nM) when compared to **4e** (IC_{50} = 8 nM).

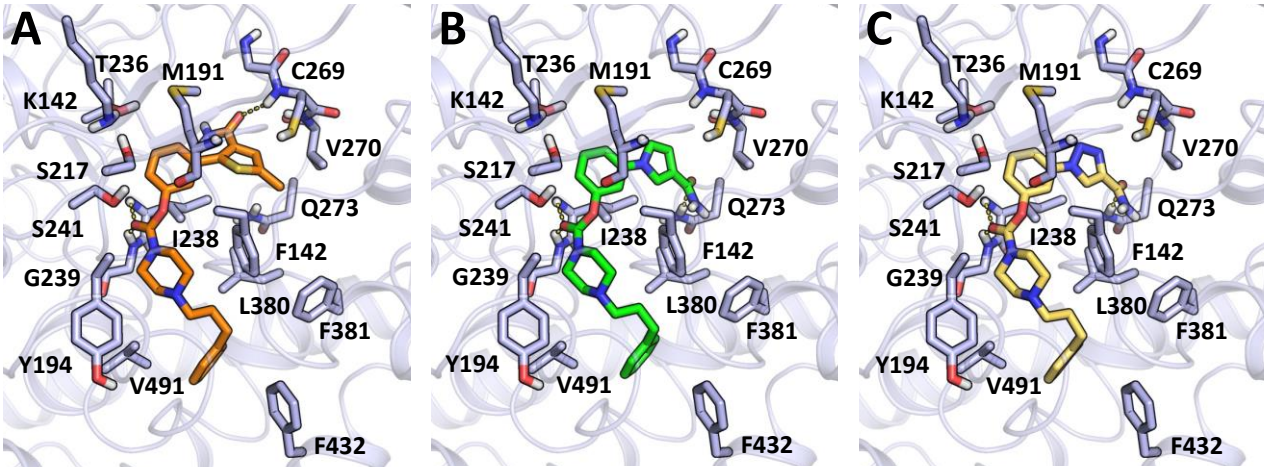

Figure 4. Best poses for compound **4k** (orange carbon atoms, panel A), **4n** (green carbon atoms, panel B) and **4p** (yellow carbon atoms, panel C) docked into FAAH (light violet carbon atoms) in neutral form. The residues of the catalytic Lys142-Ser217-Ser241 triad are also displayed. Polar interactions with CA channel residues (Cys269 or Gln273) are highlighted with dotted yellow lines.

Our SAR exploration continued investigating the importance of the peripheral 5-methylfuran-3-carboxamide on FAAH inhibitory potency by replacing it with different substituted heterocycles: *i.* 5-methylthiophene-3-carboxamide (compounds **4i-k**), *ii.* 1*H*-pyrrole-3-carboxamide (**4l-n**) and *iii.* 1*H*-1,2,3-triazole-4-carboxamide (**4o-p**). Gathered data suggest that all these substitutions were essentially bioisosteric replacements, as indicated by the activity of 4-(3-phenylpropyl)piperazine derivatives **4e, 4k, 4n**, and **4p**, displaying IC_{50} values in the medium-low nanomolar range (8.3-47 nM). Docking simulations indicated that all these compounds assumed a comparable pose within FAAH active site, and they were able to undertake similar polar interactions with the CA channel (Figure 4).

As a final step of our SAR investigation, we evaluated the impact of inserting an acid group on the aryl substituent at the oxygen atom on inhibitory potency. In the cases of arylfuran derivatives **2b** and **4e**, replacement of the 3-carbamoyl with a 3-carboxylic acid had an opposite effect. In the first case, a significant improvement of the inhibitory potency was observed, with compound **4q** displaying an IC_{50} value of 10.5 nM, 10-fold lower than that of parent compound **2b**. In the second one, a significant drop in the inhibitory potency was observed, with compound **4r**

displaying an IC_{50} value 15-fold higher than that of parent compound **4e**. When the *1H*-pyrrole-3-carboxamide fragment of **2a** and **4n** was replaced by a *2H*-tetrazol-5-yl group, a loss of inhibitory potency was observed in both cases. While for **4s** the unfavorable effect on the IC_{50} was moderate, in the case of **4t** it was considerable. We speculate that the simultaneous presence of basic and acidic functions, like in the compounds **4r** and **4t**, could generate zwitterionic species not well accommodate in the FAAH binding pocket.

The present exploration thus allowed us to identify several candidates with fair potency (IC_{50} < 100 nM) potentially endowed with higher solubility and/or enhanced chemical stability compared to reference inhibitors **2b** and **2a**, and devoid of significant activity on MAGL.

*2.3 Mechanism of action of carbamate-based FAAH inhibitors **4e**, and **4g***

To investigate the inhibition mechanism of two of the most interesting compounds, **4e** and **4g**, rapid dilution assays were performed. The compounds were incubated at two different concentrations (10 and 100 nM) in the presence of a 50-fold higher amount of FAAH than in standard conditions. After a 50-fold dilution, the substrate was added, and the enzymatic activity was evaluated. In the case of reversible inhibitors, rapid dilution disrupts the equilibrium between the inhibitor and the enzyme, resulting in enzymatic activity recovery. In contrast, dilution of the assay mixture containing the enzyme and an irreversible inhibitor would not lead to the recovery of enzymatic activity. After rapid dilution, a virtually complete recovery of FAAH activity was observed for both compounds **4e** (Figure 5A) and **4g** (Figure 5B) when compared to standard incubation conditions. These results suggest that derivatives **4e** and **4g** inhibit FAAH through a reversible mechanism. In contrast, using **1**, a known irreversible inhibitor of FAAH, no recovery of enzyme activity was observed following rapid dilution (Figure 5C).

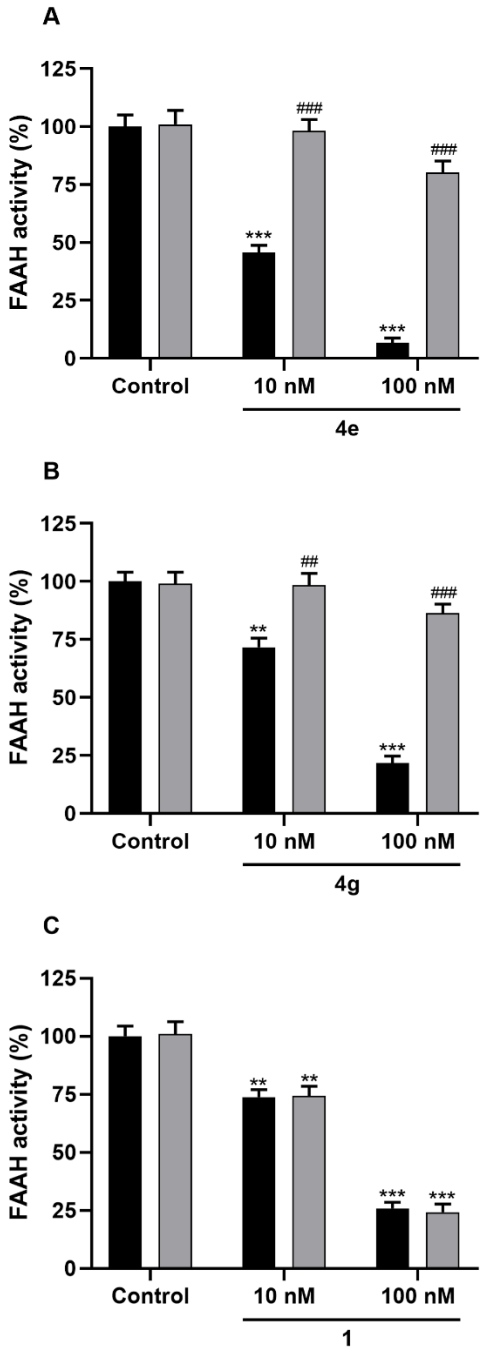

Figure 5. Reversibility of FAAH inhibition by compounds **4e** (A) and **4g** (B) in comparison to reference compound **1** (C). For the rapid dilution assay (gray histograms), FAAH activity was tested following incubation of the enzyme (50-fold concentrated) in the absence (control) or presence of the examined compounds at the 10 and 100 nM concentrations for 30 min followed by a 50-fold dilution of the assay mixture. The same compound concentrations were also assayed using the standard protocol (black histograms), and FAAH activity was then determined. The complete recovery of the enzymatic activity following rapid dilution demonstrates the reversible nature of the inhibition of compounds **4e** and **4g**. Conversely, the lack of recovery of FAAH activity confirms that the reference compound **1** act as an irreversible inhibitor. **, $p<0.01$ vs control; ***, $p<0.001$ vs control; $^{\#\#}$, $p<0.01$ vs standard protocol; $^{\#\#\#}$, $p<0.001$ vs standard protocol (two-way ANOVA followed by Tuckey's multiple comparison test).

2.4 Evaluation of chemical stability and solubility profile

In this work, our efforts were also directed on the optimization of the drug-like properties of the novel FAAH inhibitors. To achieve this aim, we inserted specific basic lateral chains or acidic moieties in the byarilic scaffolds to study their effects on water solubility and chemical stability. These data were evaluated by using HPLC method at pH 3 and pH 7.4 for selected compounds **4b, 4e**, **4g-h**, **4n-t** and are summarized in Table 2.

Table 2. Chemical stability and solubility of compounds **4b**, **4e**, **4g-h**, **4n-t**.

Cmpd	**Structure**	**IC_{50} (nM) *h*FAAH**[a]	**Stability%** pH 3, 24 h	**Stability%** pH 7.4, 24 h	**Solubility** pH 3, 24 h (µM)	**Solubility** pH 7.4, 24 h (µM)
4b	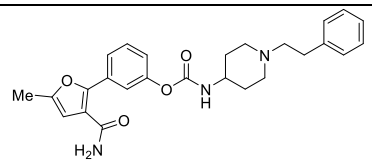	188 ± 11	96	>99	282 ± 2	67 ± 5
4e	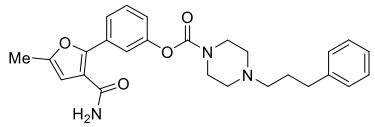	8.29 ± 0.58	98	>99	168 ± 3	<1
4g	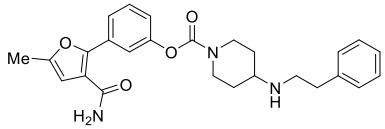	26 ± 2	>99	>99	277 ± 5	206 ± 4
4h	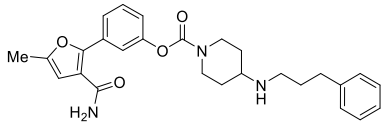	165 ± 12	>99	>99	353 ± 3	322 ± 4
4n	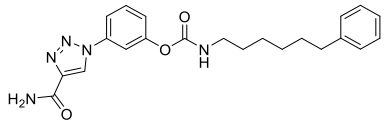	10.1 ± 0.6	>99	>99	228 ± 4	42 ± 6
4o	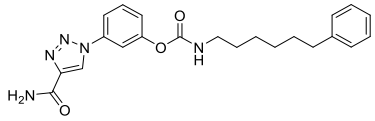	158 ± 1.1	63	79	ND[a]	ND[a]
4p	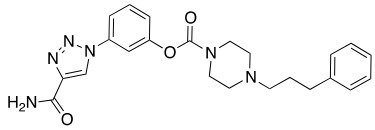	47 ± 3	>99	>99	298 ± 15	38 ± 5
4q	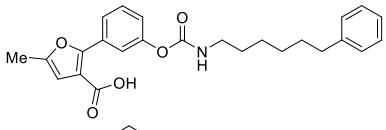	10.5 ± 0.8	<1	92.7	ND[a]	172 ± 10
4r	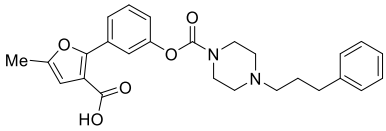	128 ± 9	>99	97	249 ± 7	259 ± 9
4s	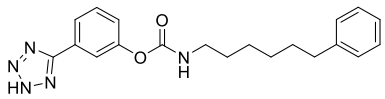	7.54 ± 0.51	<1	>99	ND[a]	108 ± 1

4t	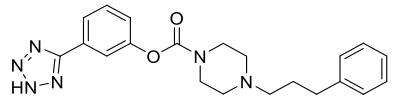	253 ± 13	>99	>99	268 ± 4	272 ± 6
2a	-	3.72 ± 0.21	32	38	3 ± 1	3 ± 1
2b	-	102 ± 9 [18]	31	9	<1[b]	<1[b]

Each value is the mean of at least three experiments; [a]ND = Not determined; [b] the data was evaluated after 12 h.

Generally, all the tested derivatives showed an excellent chemical stability at both pH values. The improved chemical stability of most of the new compounds might be due to distinct effects that disadvantage aqueous hydrolysis of the new carbamates as compared to **2a** and **2b**. These effects could be due to the increased steric hindrance in proximity of the carbamate that was obtained either by tertiarization of carbon proximal to the carbamate nitrogen (see **4b** vs **2b**, Table 2), or the tertiarization of carbamate nitrogen (see **4e** vs **2b**, Table 2). On the other hand the introduction of an acid group on leaving group as in **4q** and **4s** (see **4q** vs **2b**, and **4s** vs **2a**, Table 2) stabilized the carbamate possibly due to the presence of a negatively charged group that could disadvantage expulsion of the phenolate. The poor stability, at pH 3, of compounds **4s** and **4q** is perfectly in line with this analysis.

Improved solubility at physiological pH was obtained after insertion of a 4-aminopiperidine or a piperazine in the lateral chain of the carbamates (see **4b**, **4n**, and **4p** vs **2b**, Table 2). The notable solubility of the "inverted" 4-aminopiperidine derivatives **4g** and **4h** confirmed that the nitrogen tertiarization represents a key point for enhancing the drug disposition properties of our FAAH inhibitors particularly when associated with a secondary amine in the lateral chain that strongly increased the water solubility at pH = 7.4 up to 206 or 322 μM respectively (Table 2). The effects of acidic moieties in the biarylic portion of the inhibitors were also evaluated. The presence of a carboxylic group in the phenylhexyl derivative **4q** (Table 2) remarkably improved the water solubility at pH = 7.4 compared to the carboxamide analogue **2b**. The replacement of the carboxamido five membered heterocycle of **2a** and **2b** with a tetrazole ring, as in derivative **4s** (Table 2), allowed us to noticeably improve water solubility at pH = 7.4. We also explored the

combination of a piperazine basic lateral chain with the tetrazole or with the furane carboxylic acid moiety in compounds **4t** and **4r** that led to compounds bearing both an acidic and a basic moiety which were characterized by excellent water solubility. In line with these observations, the stability profile of compound **4o** was much lower than 90% and solubility was not measured.

2.5 Selectivity and toxicity profile

For the most promising compounds, the selectivity profile against CBR_1 and CBR_2 was evaluated, and the potential cytotoxicity was investigated in *murine* fibroblast cell lines NIH3T3 and in *human* astrocytes cell lines 1321N1. We investigated the affinity of FAAH inhibitors **4c**, **4e**, **4g**, **4k**, **4n**, **4p**, and **4s-t** towards *human* CBR_1 and CBR_2. To this aim, competition binding experiments were performed using [^{3}H]-CP-55,940 as radioligand in membranes obtained from CHO cells transfected with human CBR_1 or CBR_2. As reported in Table S1 (of the Supplementary Information), none of the selected analogues showed an affinity value (K_i) less than 10 μM for either CBRs subtypes. The cytotoxicity profile of compounds **4e**, **4g**, **4n-o**, **4s** was evaluated in the murine fibroblast cell lines (NIH3T3) after 24 h of incubation. The results, reported in Table 3, showed the low toxicity of all the selected analogues that, except for compound **4e**, nicely challenged the IC_{50} of the reference phenylfurane-based analogue **2b** by almost doubling it.

Table 3. Viability of mouse fibroblasts NIH3T3 with compounds **4e**, **4g**, **4n-o**, **4s** and reference compounds **2a** and **2b** expressed as IC_{50} (μM).

Cmpd	IC_{50} (μM)
4e	6.4
4g	45
4n	46
4o	35
4s	39
2a [21]	75
2b	19.2

Range of tested conc. for each compound = 0.6 – 180 μM.

2.5.1. Toxicity evaluation of selected compounds using the MTT assay in 1321N1 astrocytes

Furthermore, to better investigate the toxicity profile of the newly developed FAAH inhibitors, 1321N1 astrocytes viability was measured 24 h after compounds **4e**, **4n** and **4s** administration. Selected analogues displayed notable safety profile at all tested concentrations, as reported in Table 4. No toxicity was detected at all the tested concentrations (Figure S3).

Table 4. Viability of 1321N1 *human* astrocytes after compounds **4e**, **4n** and **4s** administration.

Cmpd	Cell viability (%) at different concentrations				
	10 nM	**100 nM**	**1 µM**	**10 µM**	**30 µM**
4e	99.3 ± 2.1	97.0 ± 3.0	100.0 ± 2.5	101.0 ± 2.0	96.0 ± 97.5
4n	100.5 ± 1.6	99.5 ± 1.8	100.3 ±1.7	100.0 ± 2.4	101.5 ± 1.8
4s	100.8 ± 1.5	98.5 ± 1.4	98.8 ± 1.7	99.8 ± 2.0	97.0 ± 1.5

Each value is the mean ± SEM of at least three experiments.

*2.5.2. Effect of **4n** on Langendorff perfused rat heart*

To evaluate the cardiotoxic potential of compound **4n**, its effect on cardiac mechanical function and electrocardiogram (ECG) in Langendorff-isolated rat hearts was assessed, as previously described [31,32].

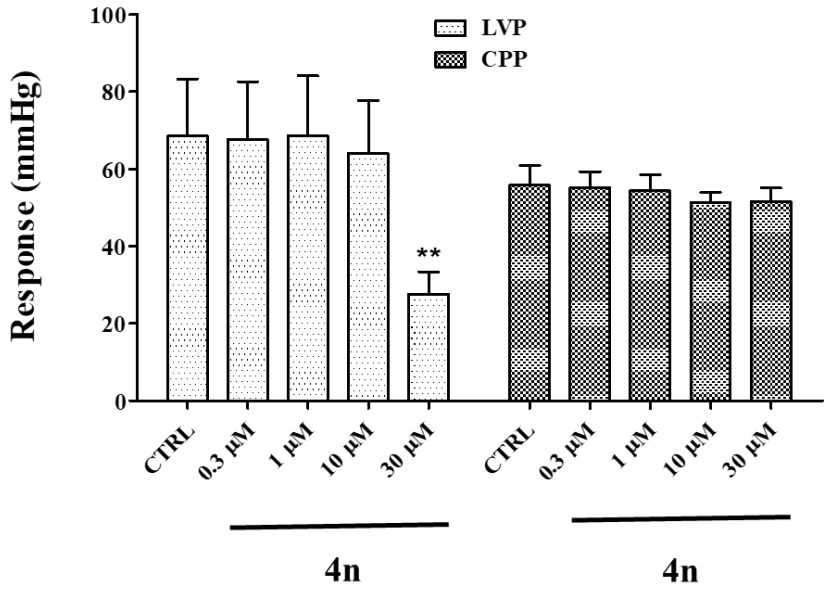

Figure 6. Effects of compound **4n** on LVP and CPP in Langendorff-perfused rat hearts. Concentration-effect relationship of compound **4n** on LVP and CPP. On the ordinate scale, the

response is reported as mmHg. Each value represents mean ± s.e.m. (n = 5). **P<0.01 vs. CTRL, repeated measures ANOVA and Dunnett's post-test.

Table 5. Effects of **4n** on HR, RR, PQ, QRS, QT, and QTc in Langendorff Perfused Rat Hearts

4n	**HR (bpm)**	**RR (ms)**	**PQ (ms)**	**QRS (ms)**	**QTc (ms)**
0	263.5 ± 8.2	230.0 ± 8.7	40.8 ± 2.3	13.6 ± 0.7	72.1 ± 1.4
0.3 μM	270.5 ± 9.3	223.8 ± 8.2	39.2 ± 2.5	13.8 ± 0.6	70.6 ± 0.8
1 μM	273.0 ± 10.5	220.2 ± 8.6	40.6 ± 2.3	13.8 ± 0.9	70.6 ± 0.9
10 μM	263.8 ± 14.0	229.8 ± 11,2	41.2 ± 2.5	14.0 ± 0.4	71.0 ± 1.6
30 μM	190.2 ± 33.9**	286.4 ± 28.7**	54.8 ± 4.1**	14.6 ± 0.6	73.5 ± 1.2

Each value represents mean ± SEM (n = 5 hearts). ** P < 0.01, repeated measures ANOVA and Dunnet post-hoc test. HR, frequency; RR, cycle length; PQ, atrioventricular conduction time; QRS, intraventricular conduction time; QTc, corrected QT (action potential duration).

Under control conditions, LVP and CPP values of 68.5 ± 14.8 and 55.8 ± 5.1 mmHg (n = 5), respectively, were obtained. At the maximum concentration tested (30 μM), **4n** significantly decreased LVP and HR, while both RR and PQ intervals were augmented (Figure 6, Table 5). However, CPP, QRS and QTc values did not vary over all the drug concentration range tested.

The present findings highlight that at the maximum concentration tested, which was three orders of magnitude higher than that effective in FAAH inhibition, **4n** exhibited negative inotropic and chronotropic activity, and prolonged the cardiac cycle length as well as the atrioventricular conduction time.

2.6. Evaluation of the anti-inflammatory profile

Although neurodegenerative diseases display different aetiology and pathogenesis, the main hallmark of these pathological conditions is represented by neuroinflammatory processes, which determine the activation of several biological mechanisms such as OS and glia responses [33]. Glia cells, including astrocytes, are involved in the maintenance of CNS homeostasis exacerbating inflammatory reactions or promoting tissue repair [15,34]. In this context ECS catabolic enzyme pharmacologic or genetic inhibition led to reduce both neuroinflammatory and neurodegenerative states in different animal models [35,36]. On these bases, we investigated the role of our new

developed FAAH inhibitors in the reduction of OS in 1321N1 *human* astrocytes cell line and determined the protective effects of our selected analogues in inflammation-induced neurodegenerated *ex vivo* cultures of rat hippocampal explants.

2.6.1 Effect of selected compound on TBHP-induced ROS production

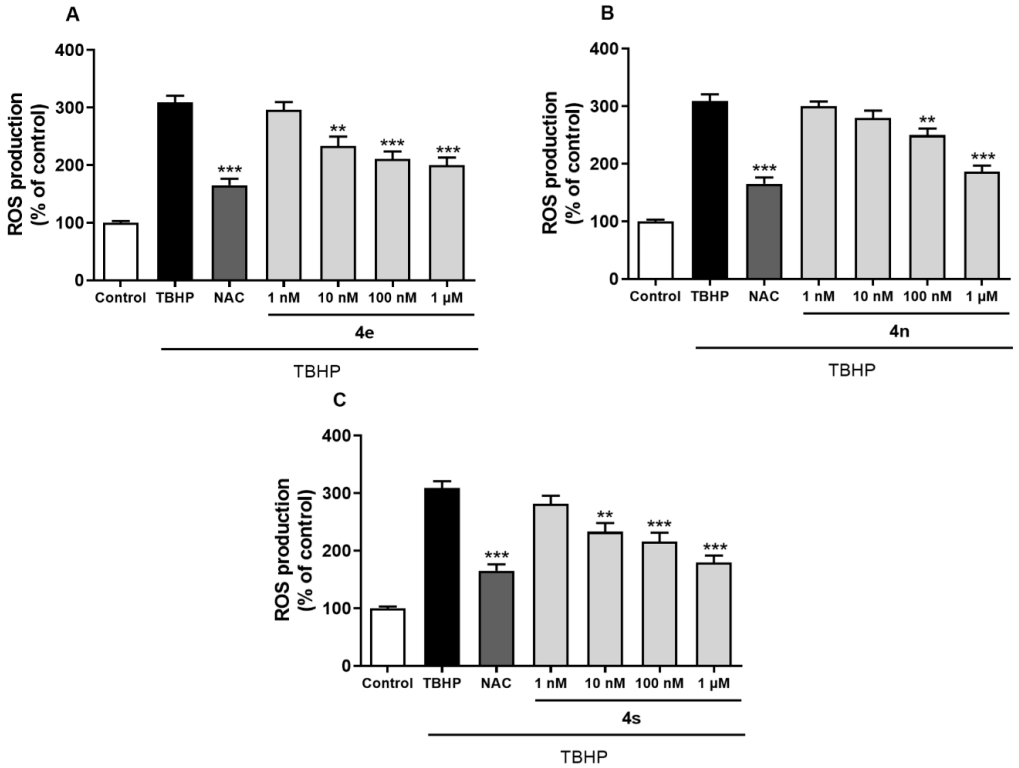

Figure 7. Effect of novel FAAH inhibitors on *tert*-butyl hydroperoxide (TBHP)-induced ROS production in 1321N1 astrocytes in comparison to NAC, 2 mM. Compound **4e** (A), **4n** (B), and **4s** (C) significantly reduced ROS levels induced by 50 µM TBHP. NAC (2 mM) was used as a reference antioxidant compound. ** $p < 0.01$ versus TBHP; *** $p < 0.001$ versus TBHP.

When administered to 1321N1 astrocytes, FAAH inhibitors **4e**, **4n**, and **4s** resulted effective in the prevention of TBHP-induced ROS production as shown in Figure 8. **4e** and **4s** significantly reduced ROS production starting from the 10 nM concentration, while compound **4n** from the 100 nM concentration. All the tested compounds at 1 µM exerted an effect similar to that of 2 mM *N*-acetylcysteine (NAC), used as a reference antioxidant compound (Figure 7).

2.6.2. Protective effect of selective FAAH inhibitors against inflammation-induced neurodegeneration in ex vivo cultures of rat hippocampal explants

To study the neuroprotective actions of FAAH inhibitors on neuroinflammatory damage, 10-12 DIV organotypic explants were exposed to a combined application of 10 μg/mL LPS and recombinant 100 ng/mL IFN-γ for 96 h, and cell death was assessed with propidium iodide (PI) staining [37]. Densitometric analysis of PI uptake revealed that when hippocampal explants were exposed to the inflammatory injury, cell death selectively occurred after 96 h in the CA1 pyramidal cell layer. The presence of **4e** (0.3 nM – 0.1 μM), **4g** (0.3 nM – 0.1 μM)**, 4n** (3 nM – 1 μM) and **4s** (0.1–10 μM) in the incubation media throughout the experiment did not affect the viability of organotypic cultures (data not shown), while significantly prevented the increase in PI uptake occurring in the CA1 region 96 h after LPS+IFN-γ exposure (Figure 8 A-D). The compound **4e** (0.3 nM – 0.1 μM) exerted dose-dependent and marked neuroprotective action in the CA1 region (70-80%) after LPS+IFN-γ exposure with an EC_{50} ~ 3 nM (EC_{50} **4e** = 2.913 nM). **4g** significantly attenuated cell death at 3 nM – 0.1 μM concentrations. **4n** significantly prevented PI uptake at concentrations of 30 nM – 1 μM. **4s** showed a significant dose-dependent protection at 1 μM and 10 μM concentrations.

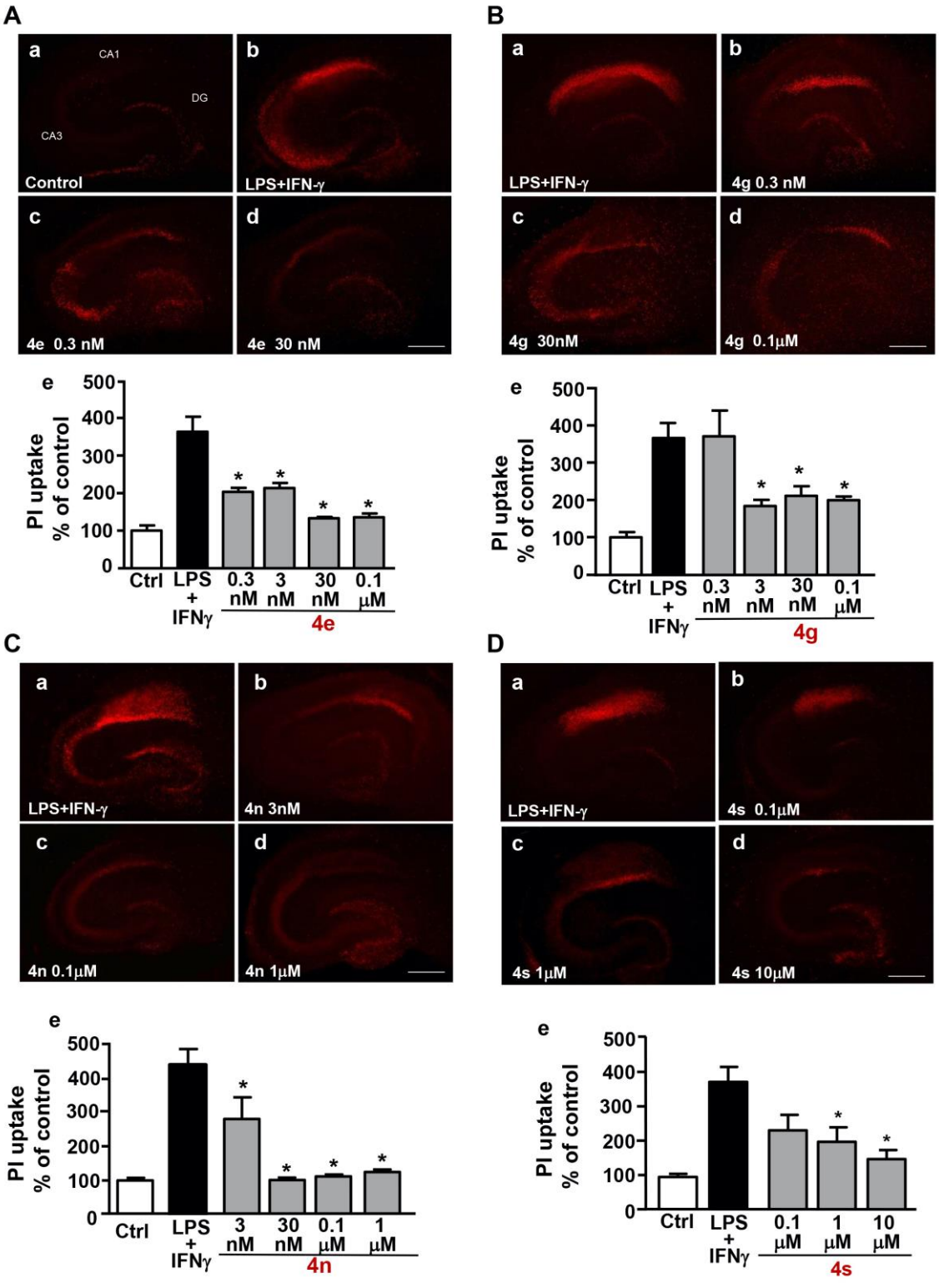

Figure 8. Effects of FAAH inhibitors against LPS+IFN-γ-induced inflammatory damage in hippocampal organotypic cultures. A–D, a-d; PI fluorescence staining patterns observed in representative hippocampal organotypic slices under control conditions (A, a) and following 96 h of LPS + IFN-γ-exposure in the absence of drug exposure (A, b; B-D, a) or in the presence of 0.3 nM – 30 nM **4e (**A, c-d); 0.3 nM – 0.1 μM **4g (**B, b-d); 3 nM – 1 μM **4n** (C, b-d); 0.1 μM – 10 μM **4s** (D, b-d). Scale bars in a-d: 500 μm. A-D, e; Quantification of cell damage in the CA1 subfield evaluated by densitometric analysis of PI fluorescence and normalized to that recorded in the CA1 subregion of untreated hippocampal slices. *$p < 0.05$ versus LPS+IFN-γ.

3. Conclusions

The cross-link between neuroinflammation and neurodegeneration is a common feature of several CNS diseases such as AD, PD, ALS and MS. The ECS plays a central role in the regulation of neuroinflammatory conditions and its indirect stimulation by using FAAH inhibitors can represent an attractive therapeutic approach to treat neuroinflammatory-based disorders. We have herein described the identification of new carbamate-based FAAH inhibitors (compounds **4a-t**) obtained by inserting ionizable functions and exploring the tertiarization of the carbamate moieties, starting from our lead compounds **2a,b**. These structure modifications allowed us to synthesize new highly potent FAAH inhibitors with an excellent selectivity profile evaluated against MAGL, CBR_1 and CBR_2. Excellent chemical stability and improved solubility over the parent compounds were demonstrated for the tested compounds. Lack of cellular toxicity for normal fibroblast cell lines was demonstrated for selected analogues, and for compound **4n** we also demonstrated absence of cardiac effects up to 30 μM concentration (when some effects appeared on cardiac parameters which however did not include alterations in CPP, QRS, and QTc values). For the most interesting analogues of the series the anti-neuroinflammatory profile was investigated. Derivatives **4e**, **4n**, and **4s** resulted effective in preventing the TBHP-induced ROS production in *human* astrocytes devoid of any toxicity effects in the same cell line as demonstrated by an MTT assay. Selected analogues **4e**, **4g**, **4n**, and **4s** resulted effective to reduce LPS + IFN-γ-interferon induced neuroinflammation in hippocampal explants. All the collected data suggest the potential use of these FAAH inhibitors as pharmacological tools for the treatment of CNS inflammatory disorders.

4. Experimental section

4.1. Chemistry

4.1.1. General procedures

All reagents were purchased from commercial suppliers and used without further purification. All moisture-sensitive reactions were performed under argon or nitrogen atmosphere using oven-dried

glassware and anhydrous solvents. Dry tetrahydrofuran (THF) was freshly distilled from sodium/benzophenone, while dichloromethane (DCM) and N,N-dimethylformamide (DMF) were freshly distilled from calcium hydride and stored under argon atmosphere. Flash column chromatography was carried out on silica gel (Merck: Kieselgel 60, particle size 0.040−0.063 mm). Reverse phase column chromatography was carried out on Lichroprep RP-18 (25−40 μm, Merck). Reactions' progression was monitored by thin- layer chromatography (TLC), carried out using glass-backed plates coated with Merck Kieselgel 60 GF254. Plates were visualized under UV light (at 254 nm) or by staining with potassium permanganate, ninhydrin, or cerium ammonium molybdate followed by heating. MW reactions were performed in a discovery microwave system (CEM).

^{1}H NMR and ^{13}C NMR spectra were recorded on a Varian 300 MHz or a Bruker 400 MHz spectrometer using the residual signal of the deuterated solvent as an internal standard. Coupling constants (J) are given in hertz (Hz). Splitting patterns are described as singlet (s), doublet (d), triplet (t), quartet (q), and broad (br); the value of chemical shifts (δ) are given in parts per million (ppm). Mass spectra were recorded utilizing an electron spray ionization (ESI) Agilent 1100 Series LC/MSD spectrometer. HRESIMS were carried out by a Thermo Finningan LCQ Deca XP Max ion-trap mass spectrometer equipped with Xcalibur software, operated in positive ion mode. Yields refer to purified products and are not optimized.

*4.1.1. 3-(2H-Tetrazol-5-yl)phenol (**5e**)*

3-Hydroxybenzonitrile **7** (200.0 mg, 1.68 mmol,), TEA hydrochloride (463.0 mg, 3.36 mmol) and sodium azide (218 mg, 3.36 mmol) were refluxed in dry toluene (17.0 mL) for 20 h. The mixture was cooled to 25 °C, diluted with water and EtOAc, and extracted with water (20.0 mL). The aqueous phase was acidified by a dropwise addition of 32% HCl until a white solid precipitated. The precipitate was filtered, washed with water and dried to give **5e** as a white solid (122 mg, 45% yield).^{1}H NMR (300 MHz, MeOD) δ 7.44 (ddt, *J* = 5.3, 2.9, 1.6 Hz, 2H), 7.37 (t, *J* = 8.0 Hz, 1H), 7.01 – 6.95 (m, 1H). ESI-MS *m*/*z* 161 [*M* -H]$^{-}$.

*4.1.2. 2-(3-Hydroxyphenyl)-5-methylfuran-3-carboxylic acid (**9**)*

To a cooled suspension of **8** (85.0 mg, 0.18 mmol) in dry DCM (3.0 mL) at -78 °C, boron tribromide, (1 M solution in DCM) (1.17 mmol, 1.10 mL) was added. The reaction was allowed to reach to 25 °C and stirred for 2 h. A saturated solution of sodium bicarbonate was added, and the mixture was extracted with DCM. The water phase was treated with 1 N HCl and extracted with EtOAc (3 x 10 mL). The combined organic layers were dried over anhydrous sodium sulfate, filtered, and concentrated *in vacuo.* Title compound **9** was obtained as a white solid and used in the next step without any further purification (85.0 mg, 99% yield). ^{1}H NMR (300 MHz, MeOD) δ 7.43 – 7.37 (m, 2H), 7.20 (dd, *J* = 8.2, 7.5, 1H), 6.82 – 6.76 (m, 1H), 6.42 (s, 1H), 2.33 (s, 3H). ESI-MS *m*/*z* 217 [*M* -H]$^-$.

*4.1.3. Benzyl 2-(3-hydroxyphenyl)-5-methylfuran-3-carboxylate (**5f**)*

To a solution of **9** (46.0 mg, 0.36 mmol) in dry DMF (2mL), sodium bicarbonate (38.0 mg, 0.45 mmol) and benzyl bromide (0.56 mmol, 73 µL) were added. The reaction was allowed to reach 40 °C and was stirred for 12 h. Saturated ammonium chloride was added, and the mixture was extracted with EtOAc. The organic layer was washed two times with saturated ammonium chloride and then with brine. The organic layer was dried over anhydrous sodium sulfate, filtered, and concentrated. The crude was purified by column chromatography on silica gel (PE/EtOAc from 5:1 to 3:1) to afford the title compound as colorless oil (77.0 mg, yield 70%). ^{1}H NMR (300 MHz, $CDCl_3$) δ 7.57 – 7.45 (m, 2H), 7.42 – 7.29 (m, 5H), 7.31 – 7.18 (m, 1H), 6.86 (dd, *J* = 8.1, 2.5, 1H), 6.46 (s, 1H), 5.27 (s, 2H), 2.33 (s, 3H). ESI-MS *m*/*z* 307 [*M* -H]$^-$.

*4.1.4. 6-(4-Methylpiperazin-1-yl)hexanenitrile (**11**)*

To a solution of 1-methylpiperazine **10** (300.0 mg, 3.0 mmol) in EtOH (5.0 mL), sodium carbonate (476.0 mg, 4.5 mmol) and 6-bromohexanenitrile (1.3 mL, 3.6 mmol) were added. The resulting mixture was stirred for 12 h at 25 °C. Then, the solvent was evaporated and the crude was purified by column chromatography on silica gel (DCM/MeOH/NH_4OH 10:1:0.1) to afford the title compound as a yellow oil (144.0 mg, 25% yield) ^{1}H NMR (300 MHz, $CDCl_3$) δ 2.76 (dd, *J* = 15.8,

10.6 Hz, 8H), 2.43 (s, 3H), 2.28 (t, *J* = 7.0 Hz, 2H), 1.65 – 1.45 (m, 4H), 1.45 – 1.32 (m, 4H). ESI-MS *m*/*z* 218 $[M + Na]^+$.

*4.1.5. 6-(4-Methylpiperazin-1-yl)hexan-1-amine (**6a**)*

To a solution of **11** (144.0 mg, 0.74 mmol) in dry THF cooled at 0 °C a solution of lithium aluminum hydride 1 M in THF (184.0 µL, 1.84 mmol) was added dropwise. The reaction mixture was allowed to reach 25 °C and stirred for 1 h. A solution of 1 N sodium hydroxide was added, and the resulting mixture was filtered through a Celite® pad. The aqueous phase was extracted with EtOAc (3 x 10 mL), and the combined organic layers were dried over anhydrous sodium sulfate, filtered, and concentrated *in vacuo*. The crude was purified by column chromatography on silica gel (DCM/MeOH/NH_4OH 10:1:0.) to afford the title compound as a yellow oil (139.0 mg, 94% yield). ^1H NMR (300 MHz, $CDCl_3$) δ 2.53 (t, *J* = 6.8 Hz, 2H), 2.44 – 2.23 (m, 8H), 2.24 – 2.16 (m, 2H), 2.14 (s, 3H), 1.46 – 1.25 (m, 4H), 1.24 – 1.09 (m, 4H). ESI-MS *m*/*z* 200 $[M + H]^+$, 241 $[M + Na]^+$.

*4.1.6. tert-Butyl (1-phenethylpiperidin-4-yl)carbamate (**13**)*

To a solution of 4-Boc-amino piperidine **12** (500.0 mg, 2.50 mmol) in dry THF (10.0 mL), 2-bromo ethylbenzene (405 µL, 3.0 mmol) and TEA (1.045 mL, 7.50 mmol) were added. The reaction mixture was heated at 70 °C for 12 h. A saturated solution of sodium bicarbonate was added, and the mixture was extracted with EtOAc (3 x 10 mL). The combined organic layers were dried over sodium sulfate, filtered and concentrated. The crude was purified by column chromatography on silica gel (PE/EtOAc from 3:1 to 1:1) to afford the title compound as an amorphous yellow solid (676 mg, 88% yield). ^1H NMR (300 MHz, $CDCl_3$) δ 7.31 – 7.23 (m, 2H), 7.22 – 7.14 (m, 3H), 3.59 – 3.38 (m, 1H), 2.99 – 2.86 (m, 4H), 2.85 – 2.72 (m, 2H), 2.62 – 2.51 (m, 2H), 2.20 – 2.06 (m, 2H), 2.01 – 1.88 (m, 2H), 1.44 (s, 9H). ESI-MS *m*/*z* 305 $[M + H]^+$, 327 $[M + Na]^+$.

*4.1.7. 1-Phenethylpiperidin-4-amine (**6b**)*

To a solution of **13** (484.0 mg, 1.5 mmol) in dry DCM (38.0 mL) cooled to 0 °C, TFA (1.3 mL) was added dropwise. The reaction mixture was allowed to reach 25 °C and stirred for 2 h under N_2 atmosphere. A saturated solution of sodium bicarbonate was added, and the mixture was extracted

with DCM (3 x 10 mL). The combined organic layers were washed with brine, dried over anhydrous sodium sulfate, filtered and concentrated. Title compound was used in the next step without any further purification (yellow oil, 290.0 mg, 95% yield). ^{1}H NMR (300 MHz $CDCl_3$) δ 7.31 – 7.23 (m, 2H), 7.21 – 7.14 (m, 3H), 2.98-2.92 (m, 2H), 2.84 – 2.75 (m, 3H), 2.63 – 2.55 (m, 2H), 2.54 – 2.42 (m, 2H), 2.14 – 2.03 (m, 2H), 1.90 – 1.78 (brs, 2H), 1.52 – 1.37 (m, 2H). ESI-MS *m*/*z* 227 $[M + Na]^+$.

*4.1.8. tert-Butyl 4-(((benzyloxy)carbonyl)amino)piperidine-1-carboxylate (**15**)*

To a mixture of compound **14** (200.0 mg, 0.98 mmol) in THF (2.5 mL) and water (1.0 mL) cooled at 0 °C sodium bicarbonate (252.0 mg, 2.97 mmol) and benzyl chloroformate (1.17 mmol, 185 μL) were added. The resulting mixture was allowed to reach 25 °C and stirred for 12 h. Water was added, and the mixture was extracted with EtOAc (3 x 10 mL). The combined organic layers were dried over sodium sulfate, filtered and concentrated. The crude was purified by column chromatography on silica gel (DCM/MeOH from 40:1 to 20:1) to afford the title compound as a colorless oil (266 mg, 80% yield) ^{1}H NMR (300 MHz, $CDCl_3$) δ 7.42 – 7.28 (m, 5H), 5.08 (s, 2H), 4.79 (brs, 1H), 3.99 (d, *J* = 13.6 Hz, 2H), 3.71 – 3.57 (m, 1H), 2.90 – 2.77 (m, 2H), 1.95 – 1.85 (m, 2H), 1.44 (s, 9H), 1.33 – 1.25 (m, 2H). ESI-MS *m*/*z* 335 $[M + H]^+$; 357 $[M + Na]^+$.

*4.1.9. Benzyl piperidin-4-ylcarbamate (**16**)*

The title compound was obtained following the procedure described for the compound **6b**, starting from compound **15** (226.0 mg, 0.68 mmol), TFA (600 μL), in dry DCM (17.0 mL). Compound **16** was obtained as a yellow oil (156.0 mg, 99% yield). ^{1}H NMR (300 MHz, $CDCl_3$) δ 7.41 – 7.14 (m, 5H), 5.03 (s, 2H), 3.70 – 3.38 (m, 1H), 3.03 – 2.94 (m, 2H), 2.72 – 2.45 (m, 2H), 1.87 (d, *J* = 9.8 Hz, 2H), 1.40 – 1.09 (m, 2H). ESI-MS *m*/*z* 235 $[M + H]^+$; 257 $[M + Na]^+$.

*4.1.10. 3-Phenylpropanal (**18**)*

To a solution of 3-phenylpropan-1-ol **17** (100.0 mg, 0.73 mmol, 100 μL), in dry DCM cooled to 0 °C, TCICA (180.0 mg, 0.77 mmol) and TEMPO (1.0 mg, 0.0074 mmol) were added. The reaction was stirred for 10 minutes at 0 °C, then the mixture was filtered through a Celite® pad and washed

with DCM. The filtrate was then washed with sodium bicarbonate (saturated solution) and then with 1 N HCl. The organic layer was dried over anhydrous sodium sulfate, filtered, and concentrated *in vacuo*. Title compound was obtained as a colorless oil and it was used in the next step without any further purification. (156.0 mg, 99% yield). ^{1}H NMR (300 MHz, (Acetone-d_6) δ 9.77 (s, 1H), 7.35 – 7.14 (m, 5H), 2.93 (t, *J* = 7.2 Hz, 2H), 2.77 (t, *J* = 7.8 Hz, 2H).

*4.1.11. Benzyl (1-(3-phenylpropyl)piperidin-4-yl)carbamate (**19**)*

To a solution of **16** (32.0 mg, 0.14 mmol) and aldehyde **18** (17.0 mg, 0.12 mmol) in dry DCM cooled at 0 °C, $NaBH(OAc)_3$ (39.5 mg, 0.19 mmol) was added. The reaction was allowed to reach 25 °C and stirred for 12 h. A saturated solution of sodium bicarbonate was added, and the mixture was extracted with DCM (3 x 10 mL). The combined organic layers were dried over anhydrous sodium sulfate, filtered, and concentrated *in vacuo.* The crude was purified by column chromatography on silica gel (DCM/MeOH from 40:1 to 20:1) to afford the title compound as a colorless oil (28.0 mg, 66% yield). ^{1}H NMR (300 MHz, $CDCl_3$) δ 7.45 – 7.07 (m, 10H), 5.08 (s, 2H), 4.72 (d, *J* = 8.1 Hz, 1H), 3.67 – 3.43 (m, 1H), 2.96 – 2.75 (m, 2H), 2.62 (t, *J* = 7.7 Hz, 2H), 2.46 – 2.30 (m, 2H), 2.10 (t, *J* = 11.4 Hz, 2H), 2.02 – 1.89 (m, 2H), 1.83 – 1.78 (m, 2H), 1.62 – 1.38 (m, 2H). ESI-MS *m*/*z* 375 $[M + Na]^+$.

*4.1.12. 1-(3-Phenylpropyl)piperidin-4-amine (**6c**)*

To a solution of compound **19** (28.0 mg, 0.08 mmol) in a mixture of EtOAc (1.5 mL) and MeOH (1.5 mL) a catalytic amount of 10% Pd on carbon was added. The resulting mixture was stirred for 2 h under H_2 atmosphere. Thereafter, the mixture was filtered and evaporated. The title compound, obtained as a yellow oil, was used in the next step without any further purification (12.0 mg, 75% yield).^{1}H NMR (300 MHz, $CDCl_3$) δ 7.51 – 6.93 (m, 5H), 2.86 – 2.80 (m, 2H), 2.75 – 2.49 (m, 5H), 2.41 – 2.26 (m, 2H), 1.98 (t, *J* = 10.4 Hz, 2H), 1.89 – 1.70 (m, 4H), 1.53 – 1.32 (m, 2H). ESI-MS *m*/*z* 241 $[M + Na]^+$.

*4.1.13. N-Methyl-1-phenethylpiperidin-4-amine (**6e**)*

To a suspension of $LiAlH_4$ (67.0 mg, 1.76 mmol) in dry THF (1.0 mL) 0 °C, a solution of compound **13** (0.32 mmol in 1 mL of dry THF) was added. The mixture was heated at 70 °C for 18 h under N_2 atmosphere. A 2 N solution of NaOH was added, and the mixture was filtered through a Celite® pad and washed with EtOAc. The separated organic layer was dried over sodium sulfate, filtered and concentrated. The crude was purified by column chromatography on silica gel (DCM/MeOH from 20:1 to 10:1) to afford the title compound as a yellow oil (113 mg, 63% yield). ^{1}H NMR (300 MHz, $CDCl_3$) δ 7.26 (dd, *J* = 8.9, 5.6 Hz, 2H), 7.22 – 7.11 (m, 3H), 3.02 – 2.87 (m, 2H), 2.84 – 2.72 (m, 2H), 2.71 – 2.62 (m, 1H), 2.61 – 2.49 (m, 2H), 2.12 – 1.95 (m, 2H), 1.93 (s, 3H), 1.89 – 1.76 (m, 2H), 1.55 – 1.29 (m, 2H). ESI-MS *m*/*z* 241 $[M + Na]^+$.

*4.1.14. (3-Bromopropyl)benzene (**20**)*

To a solution of **17** (500.0 mg, 3.80 mmol) in dry DCM, PPh_3 (1.600 g, 6.08 mmol), 1-*H*-imidazole (387.0 mg, 5.7 mmol) and CBr_4 (1.380 g, 4.18 mmol) were added. The mixture was stirred for 12 h at 25 °C. After this time water was added and the reaction was extracted with DCM (3 x 20 mL), dried over sodium sulfate, filtered and concentrated *in vacuo.* The crude was purified by column chromatography on silica gel (PE/EtOAc from 20:1 to 10:1) to afford the title compound as a colorless oil (750.0 mg, 95% yield).^{1}H NMR (300 MHz, $CDCl_3$) δ 7.35 – 7.24 (m, 2H), 7.23 – 7.15 (m, 3H), 3.40 (t, *J* = 6.6 Hz, 2H), 2.78 (t, *J* = 7.4 Hz, 2H), 2.28 – 2.09 (m, 2H).

*4.1.15. tert-Butyl 4-(3-phenylpropyl)piperazine-1-carboxylate (**21**)*

To a solution to 1-Boc-piperazine (61.0 mg, 0.33 mmol) in acetonitrile (1.5 mL) potassium carbonate (115.0 mg, 0.83 mmol), a solution of **20** (100.0 mg, 0.50 mmol) in acetonitrile (1.5 mL) and potassium iodide (cat.) were added. The reaction was stirred at 25 °C for 5 h. Then the solvent was removed, the solid residue was taken up with water and then extracted with EtOAc (3 x 20 mL). The combined organic layers were dried over sodium sulfate, filtered and concentrated *in vacuo.* The crude was purified by column chromatography on silica gel (PE/EtOAc from 2:1 to 1:1) to afford the title compound as a yellow oil (94.0 mg, 93% yield).**1**H NMR (300 MHz, $CDCl_3$) ^{1}H

NMR δ 7.31 – 7.21 (m, 2H), 7.20 – 7.13 (m, 3H), 3.50 – 3.35 (m, 4H), 2.62 (t, *J* = 7.7 Hz, 2H), 2.43 – 2.30 (m, 6H), 1.89 – 1.73 (m, 2H), 1.45 (s, 9H). ESI-MS *m*/*z* 327 $[M + Na]^+$.

*4.1.16 1-(3-Phenylpropyl)piperazine (**6f**)*

The title compound was obtained according with the procedure previously described for compound **6b**, starting from **21** (50.0 mg, 0.16 mmol) and TFA (114 µL) in dry DCM (4.0 mL). **6f** was used in the next step without any further purification (yellow oil, 28.0 mg, 99% yield). ^{1}H NMR (300 MHz, $CDCl_3$) δ 7.27 (dd, *J* = 8.6, 6.0 Hz, 2H), 7.20 – 7.13 (m, 3H), 2.90 (t, *J* = 4.9 Hz, 2H), 2.81 – 2.71 (brs, 1H), 2.62 (t, *J* = 7.7 Hz, 2H), 2.47 – 2.31 (m, 8H), 1.81 (p, *J* = 7.7, 7.3 Hz, 2H). ESI-MS *m*/*z* 205 $[M + H]^+$ 227 $[M + Na]^+$.

*4.1.17. 1-Benzylpiperidin-4-one (**23**)*

To a solution of **22** (1.000 g, 5.8 mmol) in dry DMF (10.0 mL), potassium carbonate (2.400 g, 17.4 mmol) and benzyl bromide (7.0 mmol, 835 µL) were added. The reaction was heated at 75 °C for 12 h. Then, the reaction was allowed to reach 25 °C and a saturated solution of ammonium chloride was added. The mixture was extracted with EtOAc (2 x 20 mL) and the combined organic layers were washed with ammonium chloride saturated solution (2 x 10 mL) and with brine (2 x 10 mL). The organic phase was dried over anhydrous sodium sulfate, filtered, and concentrated *in vacuo.* The crude was purified by column chromatography on silica gel (PE/EtOAc 5:1) to afford the title compound as a yellow oil (773.0 mg, 70% yield). ^{1}H NMR (300 MHz, $CDCl_3$) δ 7.36 – 7.09 (m, 5H), 3.50 (s, 2H), 2.61 (t, *J* = 6.1 Hz, 4H), 2.32 (t, *J* = 6.1 Hz, 4H). ESI-MS *m*/*z* 212 $[M + Na]^+$.

*4.1.18. Triphenyl(3-phenylpropyl)phosphonium bromide (**24**)*

To a solution of compound **20** (412.0 mg, 2.07 mmol) in dry toluene (4.0 mL), triphenylphosphine (545.0 mg, 2.07 mmol) was added. The reaction mixture was heated at 110 °C and was stirred for 48 h at this temperature. The mixture was allowed to reach 25 °C then, it was filtered, and the obtained white solid was washed several times with toluene. The solvent residue was removed *in vacuo.* Title compound was obtained as a white solid and used in the next step without any further

purification (241.0 mg, 26% yield). ^{1}H NMR (300 MHz, $CDCl_3$) δ 7.92 – 7.55 (m, 15H), 7.35 – 7.01 (m, 5H), 3.93 – 3.48 (m, 2H), 2.96 (t, *J* = 7.2 Hz, 2H), 1.90 (p, *J* = 7.6 Hz, 2H).

*4.1.19. 1-Benzyl-4-(3-phenylpropylidene)piperidine (**25**)*

To a solution of the Wittig salt **24** (245.0 mg, 0.53 mmol) in dry THF (2.0 mL) cooled at 0 °C, a solution of *n*-butyl lithium (1.6 M in hexane, 280 µL, 0.44 mmol) was added and the resulting mixture was stirred for 2 h at this temperature. Then a solution of ketone **23** in dry THF (1.0 mL) was added dropwise at 0 °C. The reaction was allowed to reach 25 °C and it was stirred for 12 h. A saturated solution of ammonium chloride was added, and the mixture was extracted with EtOAc (3 x 10 mL). The combined organic layers were dried over anhydrous sodium sulfate, filtered, and concentrated *in vacuo.* The crude was purified by column chromatography on silica gel (PE/EtOAc 5:1) to afford the title compound as a colorless oil (43.0 mg, 28% yield). ^{1}H NMR (300 MHz, $CDCl_3$) δ 7.37 – 7.20 (m, 7H), 7.21 – 7.10 (m, 3H), 5.20 – 5.13 (m, 1H), 3.50 (s, 2H), 2.69 – 2.57 (m, 2H), 2.40 (t, *J* = 5.7 Hz, 2H), 2.34 – 2.24 (m, 4H), 2.22 – 2.14 (m, 4H). ESI-MS *m*/*z* 314 [*M* +Na]$^+$.

*4.1.20. 4-(3-Phenylpropyl)piperidine (**6g**)*

The title compound was obtained following the procedure described for compound **6c**, starting from amine **25** (18.0 mg, 0.06 mmol) in a mixture of EtOAc (1.0 mL) and MeOH (1.0 mL). The title compound was obtained as a yellow oil and was used in the next step without any further purification (10 mg, 82% yield). ^{1}H NMR (300 MHz, $CDCl_3$) δ 7.73 – 7.38 (m, 2H), 7.37 – 6.83 (m, 3H), 5.71 – 5.07 (brs, 1H), 3.28 (d, *J* = 11.8 Hz, 2H), 2.81 – 2.44 (m, 4H), 1.97 – 1.52 (m, 4H), 1.48 – 1.12 (m, 5H). ESI-MS *m*/*z* 226 [*M* +H]$^+$.

*4.1.21. tert-Butyl 4-(phenethylamino)piperidine-1-carboxylate (**27**)*

The title compound was obtained following the procedure described for compound **19**, starting from **26** (300.0 mg, 1.51 mmol), phenylethylamine (208.63 µL, 1.66 mmol) and $NaBH(OAc)_3$ (478.0 mg, 2.26 mmol) in dry DCM (22.0 mL). The crude was purified by column chromatography on silica gel (DCM/MeOH from 40:1 to 20:1) to afford the title compound as a colorless oil (287 mg, 62%

yield). ^{1}H NMR (300 MHz, $CDCl_3$) δ 7.30 – 7.10 (m, 5H), 3.98 (s, 2H), 2.91 – 2.81 (m, 2H), 2.80 – 2.67 (m, 4H), 2.56 (m, 1H), 1.83 – 1.71 (m, 2H), 1.41 (s, 9H), 1.31 – 1.09 (m, 3H). ESI-MS *m*/*z* 327 $[M + Na]^+$.

*4.1.22. tert-Butyl 4-(((benzyloxy)carbonyl)(phenethyl)amino)piperidine-1-carboxylate (**28**)*

The title compound was obtained following the procedure described for compound **15**, starting from **27** (286.0 mg, 0.94 mmol), benzyl chloroformate (174.0 μL, 1.2 mmol) and sodium bicarbonate (237.0 mg, 2.8 mmol) in THF (2.5 mL) and water (1.0 mL).The crude was purified by column chromatography on silica gel (PE/EtOAc from 5:1 to 3:1) to afford the title compound as a colorless oil (410.0 mg, 99% yield).^{1}H NMR (300 MHz, $CDCl_3$) δ 7.59 – 6.94 (m, 10H), 5.18 (s, 2H), 4.28 – 4.05 (m, 3H), 3.46 – 3.21 (m, 2H), 2.99 – 2.60 (m, 4H), 1.77 – 1.50 (m, 4H), 1.48 (s, 9H). ESI-MS *m*/*z* 461 $[M + Na]^+$.

*4.1.23. Benzyl phenethyl(piperidin-4-yl)carbamate (**6h**)*

The title compound was obtained follow the procedure described for the compound **6b,** starting from **28** (410.0 mg, 0.94 mmol) and TFA (300 μL), in dry DCM (30.0 mL). Compound **6h** was obtained as a yellow oil (276.0 mg, 87% yield). ^{1}H NMR (300 MHz, CD_3OD) δ 7.74 – 6.64 (m, 10H), 4.91 (s, 2H), 3.96 – 3.90 (m, 1H), 3.52 – 3.33 (m, 4H), 3.00 (t, *J* = 12.6 Hz, 2H), 2.90 – 2.76 (m, 2H), 2.34 – 1.92 (m, 2H), 1.77 (d, *J* = 13.6 Hz, 2H). ESI-MS m/z 361 $[M + Na]^+$.

*4.1.24. tert-Butyl 4-((3-phenylpropyl)amino)piperidine-1-carboxylate (**29**)*

The title compound was obtained following the procedure described for compound **19**, starting from **14** (153.0 mg, 0.76 mmol), aldehyde **18** (93.0 mg, 0.69 mmol) and $NaBH(OAc)_3$ (220.0 mg, 1.0 mmol) in dry DCM (10.0 mL). The crude was purified by column chromatography on silica gel (DCM/MeOH from 40:1 to 20:1) to afford the title compound as a yellow oil (131.0 mg, 60% yield). ^{1}H NMR (300 MHz, $CDCl_3$) δ 7.31 – 7.09 (m, 5H), 4.05-3.93 (m, 2H), 2.88 – 2.45 (m, 7H), 1.93 – 1.71 (m, 4H), 1.42 (s, 9H), 1.32 – 1.11 (m, 2H). ESI-MS *m*/*z* $[M + Na]^+$ 341.

*4.1.25. tert-Butyl 4-(((benzyloxy)carbonyl)(3-phenylpropyl)amino)piperidine-1-carboxylate (**30**)*

The title compound was obtained following the procedure described for compound **15**, starting from **29** (131.0 mg, 0.41 mmol), benzyl chloroformate (91.2 mg, 0.54 mmol) and sodium bicarbonate (91.3 mg, 0.54 mmol) in THF (1.0 mL) and water (500 µL). The crude was purified by column chromatography on silica gel (PE/EtOAc from 5:1 to 3:1) to afford the title compound as a colorless oil (165.0 mg, 88% yield).^{1}H NMR (300 MHz, $CDCl_3$) δ 7.47 – 7.03 (m, 10H), 5.14 (s, 2H), 4.33 – 4.02 (m, 3H), 3.34 – 3.02 (m, 2H), 2.86 – 2.44 (m, 4H), 1.99 – 1.75 (m, 2H), 1.72 – 1.51 (m, 4H), 1.48 (s, 9H). ESI-MS *m*/*z* $[M + Na]^+$ 475.

*4.1.26. Benzyl (3-phenylpropyl)(piperidin-4-yl)carbamate (**6i**)*

The title compound was obtained following the procedure described for the compound **6b,** starting from **30** (165 mg, 0.37 mmol) and TFA (330 µL) in dry DCM (9.0 mL). After purification, compound **6i** was obtained as a yellow oil (130.0 mg, 99% yield). ^{1}H NMR (300 MHz, $CDCl_3$) δ 7.55 – 7.00 (m, 10H), 5.13 (s, 2H), 4.16 – 3.92 (brs, 1H), 3.33 – 2.96 (m, 4H), 2.74 – 2.48 (m, 4H), 2.46 – 2.37 (m, 1H), 1.96 – 1.79 (m, 2H), 1.75 – 1.50 (m, 4H). ESI-MS *m*/*z* 375 $[M + Na]^+$.

*4.1.27. 3-(3-Carbamoyl-5-methylfuran-2-yl)phenyl-(((benzyloxy)carbonyl)(phenethyl)amino)piperidine-1-carboxylate (**31a**)*

To a solution of **5a** (18.0 mg, 0.083 mmol) in dry DCM (4.0 mL) under N_2 atmosphere cooled to 0 °C, TEA (34 µL, 0.25 mmol) and 4-nitrophenyl chloroformate (25.0 mg, 0.12 mmol) were added. The mixture was kept for 2 h at 0 °C. After this time, a solution of the amine **6h** (41.0 mg, 0.12 mmol) in dry DCM (1.5 mL) was added. The reaction was allowed to reach 25 °C and was stirred for 2 h. Water was added, and the mixture was extracted with DCM (3 x 10 mL). The combined organic layers were dried over sodium sulfate, filtered and concentrated. The crude was purified by column chromatography on silica gel (DCM/MeOH from 90:1 to 70:1) to afford the title compound as a colorless oil (31.0 mg, 64% yield). ^{1}H NMR (300 MHz, $CDCl_3$) δ 7.67 (dd, *J* = 7.8, 1.7, Hz, 1H), 7.62 – 7.55 (m, 1H), 7.49 – 7.24 (m, 5H), 7.31 – 7.15 (m, 4H), 7.16 – 7.04 (m, 3H), 6.31 (s, 1H), 5.79 (brs, 2H), 5.19 (s, 2H), 4.48 – 4.27 (m, 2H), 4.22 – 4.17 (m, 1H), 3.43 – 3.30 (m, 2H), 3.14 – 2.77 (m, 4H), 2.33 (s, 3H), 1.82 – 1.62 (m, 4H). ESI-MS *m*/*z* 604 $[M + Na]^+$.

*4.1.28. 3-(3-Carbamoyl-5-methylfuran-2-yl)phenyl 4-(((benzyloxy)carbonyl)(3-phenylpropyl)amino)piperidine-1-carboxylate (**31b**)*

The title compound was prepared according with the procedure described for **31a**, starting from **5a** (15.0 mg, 0.07 mmol), 4-nitrophenyl chloroformate (21.0 mg, 0.10 mmol), TEA (30.0 µL, 0.21 mmol) amine **6i** (36.5 mg, 0.10 mmol) in dry DCM (6.0 mL). The crude was purified by column chromatography on silica gel (DCM/MeOH from 70:1 to 60:1) to afford the title compound as an amorphous white solid (21.0 mg, 51% yield). ^{1}H NMR (300 MHz, $CDCl_3$) δ 7.76 – 7.53 (m, 2 H), 7.49 – 7.02 (m, 12 H), 6.32 (s, 1H), 5.76 – 5.59 (brs, 2H), 5.15 (s, 2H), 4.35 (t, *J* = 15.0 Hz, 2H), 4.23 – 4.04 (m, 1H), 3.34 – 3.08 (m, 2H), 3.06 – 2.80 (m, 2H), 2.68 – 2.46 (m, 2H), 2.34 (s, 3H), 2.00 – 1.60 (m, 6H). ESI-MS *m*/*z* 596 $[M + H]^+$; 618 $[M + Na]^+$.

*4.1.29. Benzyl 5-methyl-2-(3-(((6-phenylhexyl)carbamoyl)oxy)phenyl)furan-3-carboxylate (**32**)*

The title compound was prepared according to the procedure described for **31a**, starting from **5f** (77.0 mg, 0.25 mmol), 4-nitrophenyl chloroformate (74.0 mg, 0.37 mmol), TEA (104 µL, 0.75 mmol) and amine **6d** (65.0 mg, 0.37 mmol) in dry DCM (9.0 mL). The crude was purified by column chromatography on alumina gel (PE/EtOAc 8:1 to 5:1) to afford the title compound as an amorphous white solid (21.0 mg, 16% yield). ^{1}H NMR (300 MHz, $CDCl_3$) δ 7.92 – 7.76 (m, 1H), 7.54 – 7.47 (m, 1H), 7.41 – 7.10 (m, 11H), 6.89 – 6.77 (m, 1H), 6.46 (s, 1H), 5.27 (s, 2H), 5.03 (t, *J* = 5.8 Hz, 1H), 3.31 – 3.20 (m, 2H), 2.65 – 2.56 (m, 2H), 2.33 (s, 3H), 1.71 – 1.49 (m, 4H), 1.43 – 1.34 (m, 4H). ESI-MS *m*/*z* 534 $[M + Na]^+$.

*4.1.30. 3-(3-((Benzyloxy)carbonyl)-5-methylfuran-2-yl)phenyl 4-(3-phenylpropyl)piperazine-1-carboxylate (**33**)*

The title compound was prepared according to the procedure described for **31a**, starting from **5f** (42.0 mg, 0.13 mmol), 4-nitrophenyl chloroformate (40.0 mg, 0.20 mmol), TEA (57 µL, 0.40 mmol) and amine **6f** (42.0 mg, 0.20 mmol) in dry DCM (6.0 mL). The crude was purified by column chromatography on alumina gel (PE/EtOAc 4:1 to 2:1) to afford the title compound as an amorphous white solid (21.0 mg, 64% yield). ^{1}H NMR (300 MHz, $CDCl_3$) δ 7.88 (dd, *J* = 7.9, 1.3

Hz, 1H), 7.77 (t, *J* = 2.0 Hz, 1H), 7.45 – 7.08 (m, 12H), 6.46 (d, *J* = 1.3 Hz, 1H), 5.28 (s, 2H), 3.67 (d, *J* = 28.6 Hz, 4H), 2.68 (t, *J* = 7.7 Hz, 2H), 2.58 – 2.40 (m, 6H), 2.33 (s, 3H), 1.94 – 1.81 (m, 2H).

*4.1.31. 3-(3-Carbamoyl-5-methylfuran-2-yl)phenyl (6-(4-methylpiperazin-1-yl)hexyl)carbamate (**4a**)*

The title compound was prepared according to the procedure described for **31a**, starting from **5a** (15.0 mg, 0.07 mmol), 4-nitrophenyl chloroformate (20.0 mg, 0.10 mmol), TEA (30 μL, 0.46 mmol) and amine **6a** (20.0 mg, 0.10 mmol) in dry DCM (4.0 mL). The crude was purified by column chromatography on silica gel (EtOAc/MeOH/TEA 8:1:0.1) to afford the title compound as a colorless oil (5.2 mg, 17% yield). ^{1}H NMR (300 MHz, $CDCl_3$) δ 7.73 – 7.68 (m, 1H), 7.65 (t, *J* = 2.0 Hz, 1H), 7.39 (t, *J* = 8.0 Hz, 1H), 7.10 – 7.04 (m, 1H), 6.39 (s, 1H), 3.19 (t, *J* = 6.8 Hz, 2H), 3.04 – 2.79 (m, 8H), 2.77 – 2.65 (m, 2H), 2.54 (s, 3H), 2.36 (s, 3H), 1.69 – 1.51 (m, 4H), 1.47 – 1.35 (m, 4H). ^{13}C NMR (75 MHz, $CDCl_3$) 165.7, 154.5, 151.9, 151.7, 151.0, 131.0, 129.6, 122.1, 121.1, 117.8, 108.3, 108.1, 58.7, 54.8, 52.9, 45.9, 45.7, 41.1, 29.7, 27.0, 26.5, 13.5. ESI-MS *m*/*z* 442 $[M+H]^+$.

*4.1.32. 3-(3-Carbamoyl-5-methylfuran-2-yl)phenyl (1-phenethylpiperidin-4-yl)carbamate (**4b**)*

The title compound was prepared according to the procedure described for **31a**, starting from **5a** (40.0 mg, 0.17 mmol), 4-nitrophenyl chloroformate (51.0 mg, 0.25 mmol), TEA (71 μL, 0.51 mmol) and amine **6b** (51.0 mg, 0.25 mmol) in dry DCM (14.0 mL). The crude was purified by column chromatography on silica gel (EtOAc/MeOH from 20:1 to 10:1) to afford the title compound as an amorphous white solid (38.7 mg, 51% yield). ^{1}H NMR (300 MHz, DMSO-d_6) δ 7.76 (dd, *J* = 20.2, 7.9 Hz, 2H), 7.67 (d, *J* = 8.3 Hz, 2H), 7.38 (t, *J* = 8.0 Hz, 1H), 7.31 – 7.14 (m, 5H), 7.06 (d, *J* = 8.1 Hz, 1H), 6.49 (s, 1H), 4.04 (s, 1H), 2.89 (d, *J* = 11.0 Hz, 2H), 2.74 – 2.66 (m, 2H), 2.32 (s, 3H), 2.07 – 1.89 (m, 3H), 1.84 – 1.72 (m, 2H), 1.54 – 1.40 (m, 4H). ^{13}C NMR (75 MHz, DMSO-d_6) 165.4, 153.9, 151.3, 151.2, 150.5, 141.0, 131.6, 129.5, 129.1, 128.7, 126.2, 123.5,

122.0, 120.3, 119.7, 109.0, 60.1, 52.3, 48.8, 33.4, 32.1, 29.5, 29.1, 22.5. ESI-MS *m/z* 448 $[M+H]^+$, 470 $[M + Na]^+$. HRMS(ESI) *m/z* $[M + H]^+$ calcd for $[C_{26}H_{30}N_3O_4]^+$ 448.2231, found 448.2211.

4.1.33. 3-(3-Carbamoyl-5-methylfuran-2-yl)phenyl (1-(3-phenylpropyl)piperidin-4-yl)carbamate ***(4c)***

The title compound was prepared according to the procedure described for **31a**, starting from **5a** (8.0 mg, 0.04 mmol), 4-nitrophenyl chloroformate (11.0 mg, 0.06 mmol), TEA (20 μL, 0.15 mmol) and amine **6c** (12.0 mg, 0.06 mmol) in dry DCM (2.0 mL). The crude was purified by column chromatography on silica gel (18.0 mg, 66% yield). ^{1}H NMR (300 MHz, CD_3OD) δ 7.71 (dd, *J* = 7.9, 1.7, Hz, 1H), 7.67 - 7.63 (m, 1H), 7.39 (t, *J* = 8.0 Hz, 1H), 7.32 – 7.13 (m, 5H), 7.07 – 7.03 (m, 1H), 6.39 (s, 1H), 3.72 – 3.52 (m, 1H), 3.27 – 3.16 (m, 2H), 2.81 – 2.48 (m, 6H), 2.35 (s, 3H), 2.16 – 2.01 (m, 2H), 1.98 – 1.85 (m, 2H), 1.83 – 1.63 (m, 2H). ^{13}C NMR (75 MHz, CD_3OD) δ 167.7, 154.9, 151.7, 151.2, 151.0, 140.9, 131.4, 128.8, 128.1, 128.0, 125.8, 123.6, 121.4, 120.0, 118.0, 107.7, 107.6, 56.8, 51.4, 32.7, 29.8, 26.8, 11.8, 11.8. ESI-MS *m/z* 484 $[M + Na]^+$. HRMS(ESI) *m/z* $[M + H]^+$ calcd for $[C_{27}H_{32}N_3O_4]^+$ 462.2387, found 462.2374.

4.1.34. 3-(3-Carbamoyl-5-methylfuran-2-yl)phenylmethyl-1-phenethylpiperidin-4-amine carbamate ***(4d)***

The title compound was prepared according to the procedure described for **31a**, starting from **5a** (25.0 mg, 0.11 mmol), 4-nitrophenyl chloroformate (33.0 mg, 0.16 mmol), TEA (0.33 mmol, 45 μL) and amine **6e** (32.0 mg, 0.15 mmol) in dry DCM (5.0 mL). The crude was purified by column chromatography on silica gel (EtOAc/MeOH from 50:1 to 20:1) to afford the title compound as an amorphous white solid (18.7 mg, 37% yield). ^{1}H NMR (300 MHz, CD_3OD) δ 7.74 (d, *J* = 7.9 Hz, 1H), 7.67 (s, 1H), 7.40 (t, *J* = 8.0 Hz, 1H), 7.32 – 7.14 (m, 5H), 7.12 – 7.01 (m, 1H), 6.39 (s, 1H), 4.06 (d, *J* = 18.2 Hz, 1H), 3.15 (d, *J* = 11.4 Hz, 2H), 3.02 (s, 3H), 2.94 – 2.72 (m, 2H), 2.63 (dd, *J* = 10.8, 5.7 Hz, 2H), 2.35 (s, 3H), 2.20 (s, 2H), 2.04 – 1.66 (m, 4H). ^{13}C NMR (75 MHz, CD_3OD) δ 168.6, 154.9, 151.3, 141.1, 139.7, 139.6, 134.5, 132.7, 129.1, 128.2, 128.1, 126.6, 126.54, 125.8, 125.7, 121.9, 121.3, 59.8, 52.5, 32.8, 28.2, 13.5. ESI-MS *m/z* 484 $[M + Na]^+$.

*4.1.35. 3-(3-Carbamoyl-5-methylfuran-2-yl)phenyl 4-(3-phenylpropyl)piperazine-1-carboxylate (**4e**)*

The title compound was prepared according to the procedure described for **31a**, starting from **5a** (10.0 mg, 0.04 mmol), 4-nitrophenyl chloroformate (12.0 mg, 0.06 mmol), TEA (20 μL, 0.15 mmol) amine **6f** (13.0 mg, 0.06 mmol) in dry DCM (3.0 mL). The crude was purified by column chromatography on silica gel (EtOAc/MeOH 100:1) to afford the title compound as an amorphous white solid (11.8 mg, 66% yield). ^{1}H NMR (300 MHz, $CDCl_3$) δ 7.65 (dd, *J* = 7.8, Hz, 1H), 7.56 (t, *J* = 1.9 Hz, 1H), 7.39 (t, *J* = 8.0 Hz, 1H), 7.32 – 7.23 (m, 2H), 7.22 – 7.14 (m, 3H), 7.13 – 7.06 (m, 1H), 6.32 (s, 1H), 5.92 – 5.45 (brs, 2H), 3.63 (d, *J* = 31.5 Hz, 4H), 2.66 (t, *J* = 7.7 Hz, 2H), 2.53 – 2.37 (m, 6H), 2.33 (d, *J* = 1.0 Hz, 3H), 1.84 (p, *J* = 7.6, 7.2 Hz, 2H).^{13}C NMR (75 MHz, $CDCl_3$) δ 165.2, 154.4, 152.5, 151.4, 150.6, 141.9, 131.8, 130.3, 128.4, 128.3, 126.3, 124.5, 122.9, 121.1, 118.4, 108.2, 57.8, 52.2, 44.9, 43.4, 35.6, 29.0, 16.4. ESI-MS *m/z* 470 $[M + Na]^+$. HRMS(ESI) *m/z* $[M + H]^+$ calcd for $[C_{26}H_{30}N_3O_4]^+$ 448.2231 found 448.2231, $[M + Na]^+$ calcd for $[C_{26}H_{29}N_3NaO_4]^+$ 470.2050, found 470.2041.

*4.1.36. 3-(3-Carbamoyl-5-methylfuran-2-yl)phenyl 4-(3-phenylpropyl)piperidine-1-carboxylate (**4f**)*

The title compound was prepared according to the procedure described for **31a**, starting from **5a** (7.0 mg, 0.26 mmol), 4-nitrophenyl chloroformate (8.0 mg, 0.23 mmol), TEA (10 μL, 0.46 mmol) and amine **6g** (9.0 mg, 0.04 mmol) in dry DCM (2.0 mL). The crude was purified by column chromatography on silica gel (DCM/acetone 8:1) to afford the title compound as a colorless oil (4.5 mg, 40% yield). ^{1}H NMR (300 MHz, $CDCl_3$) δ 7.63 (d, *J* = 7.5 Hz, 1H), 7.54 (d, *J* = 3.0 Hz, 1H), 7.50 – 7.36 (m, 2H), 7.27 (d, *J* = 8.3 Hz, 3H), 7.22 – 7.05 (m, 2H), 6.34 (s, 1H), 5.89 – 5.45 (brs, 2H), 4.24 (t, *J* = 18.4 Hz, 2H), 3.02 – 2.74 (m, 2H), 2.62 (t, *J* = 7.7 Hz, 2H), 2.34 (s, 3H), 1.79 – 1.59 (m, 7H), 1.33– 1.21 (m, 2H). ^{13}C NMR (75 MHz, $CDCl_3$) δ 165.6, 153.5, 151.9, 151.6, 151.2, 142.4, 130.9, 129.5, 128.4, 128.3, 125.7, 124.4, 122.3, 121.7, 121.8, 108.3, 108.2, 44.9, 44.5, 36.0, 35.8, 32.2, 31.8, 29.7, 28.5. ESI-MS *m/z* 447 $[M + H]^+$. HRMS(ESI) *m/z* $[M + H]^+$ calcd for

$[C_{27}H_{31}N_2O_4]^+$ 447.2278, found 447.2264; [*M* + Na]$^+$; calcd for $[C_{27}H_{30}N_2NaO_4]^+$ 469.2098, found 469.2079.

*4.1.37. 3-(3-Carbamoyl-5-methylfuran-2-yl)phenyl 4-(phenethylamino)piperidine-1-carboxylate (**4g**)*

The title compound was obtained according to the procedure described for compound **6c**, starting from **31a** (31.0 mg, 0.06 mmol) in a mixture of EtOAc (1.0 mL) and MeOH (2.0 mL). The crude was purified by column chromatography on silica gel (DCM/MeOH/NH_4OH 10:1:0.1) to afford the title compound as an amorphous white solid (12.0 mg, 54% yield). ^{1}H NMR (300 MHz, $CDCl_3$) δ 7.67 – 7.62 (m, 1H), 7.56 (d, *J* = 1.8 Hz, 1H), 7.42 – 7.35 (m, 1H), 7.34 – 7.25 (m, 2H), 7.25 – 7.18 (m, 3H), 7.08 (dd, *J* = 8.2, 2.5 Hz, 1H), 6.31 (s, 1H), 5.95 – 5.78 (brs, 2H), 4.28 – 4.09 (m, 2H), 3.06 (t, *J* = 12.5 Hz, 1H), 3.00 – 2.90 (m, 4H), 2.89 – 2.81 (m, 2H), 2.81 – 2.71 (m, 1H), 2.32 (s, 3H), 2.00 – 1.88 (m, 2H), 1.42 (d, *J* = 11.7 Hz, 2H). ^{13}C NMR (75 MHz, $CDCl_3$) δ 165.8, 153.5, 151.9, 151.5, 151.2, 139.4, 131.0, 129.5, 128.7, 128.6, 126.4, 124.4, 122.1, 121.1, 117.8, 108.2, 54.6, 47.8, 43.3, 43.0, 36.0, 32.0, 31.6, 13.4. ESI-MS *m/z* 470 [*M* + Na]$^+$. HRMS(ESI) *m/z* [*M* + H]$^+$ calcd for $[C_{26}H_{30}N_3O_4]^+$ 448.2231, found 448.2213.

*4.1.38. 3-(3-Carbamoyl-5-methylfuran-2-yl)phenyl 4-((3-phenylpropyl)amino)piperidine-1-carboxylate (**4h**)*

The title compound was obtained according to the procedure described for compound **6c**, starting from **31b** (21.0 mg, 0.035 mmol) in a mixture of EtOAc (1.5 mL) and MeOH (1.5 mL). The crude was purified by column chromatography on silica gel (DCM/MeOH/NH_4OH 10:1:0.1) to afford the title compound as an amorphous white solid (12.0 mg, 74% yield). ^{1}H NMR (300 MHz, $CDCl_3$) δ 7.63 (dd, *J* = 7.8, 1.7, 1H), 7.58 (dd, *J* = 2.3, 1.6 Hz, 1H), 7.38 (t, *J* = 8.0 Hz, 1H), 7.28 – 7.22 (m, 2H), 7.21 – 7.14 (m, 3H), 7.10 – 7.04 (m, 1H), 6.30 (s, 1H), 6.14 – 5.93 (m, 2H), 4.31 – 4.13 (m, 1H), 3.07 – 2.84 (m, 4H), 2.83 – 2.76 (m, 2H), 2.67 (t, *J* = 7.6 Hz, 2H), 2.32 (s, 3H), 2.07 – 1.93 (m, 5H), 1.62-158 (m, 2H).^{13}C NMR (75 MHz, $CDCl_3$) δ 166.0, 153.5, 151.9, 151.4, 151.2, 141.0, 131.1, 129.5, 128.5, 128.3, 126.1, 124.3, 122.1, 120.9, 117.8, 108.2, 54.8, 45.3, 43.2, 42.9, 33.2,

30.7, 30.2, 29.9, 13.4. ESI-MS *m/z* 484 [*M* + Na]$^+$. HRMS(ESI) *m/z* [*M* + H]$^+$ calcd for [$C_{27}H_{32}N_3O_4$]$^+$ 462.2387, found 462.2372.

*4.1.39. 3-(3-Carbamoyl-5-methylthiophen-2-yl)phenyl (1-phenethylpiperidin-4-yl)carbamate (**4i**)*

The title compound was prepared according to the procedure described for **31a**, starting from **5b** (37.0 mg, 0.16 mmol), 4-nitrophenyl chloroformate (47.0 mg, 0.23 mmol), TEA (70 µL, 0.51 mmol) and amine **6b** (46.0 mg, 0.23 mmol) in dry DCM (12.0 mL). The crude was purified by column chromatography on silica gel (EtOAc/MeOH 30:1) to afford the title compound as an amorphous white solid (28.0 mg, 38% yield). ^{1}H NMR (300 MHz, DMSO-d_6) δ 7.81 (d, *J* = 7.7 Hz, 1H), 7.60 (s, 1H), 7.36 (t, *J* = 8.0 Hz, 1H), 7.30 – 7.13 (m, 7H), 7.10 – 7.02 (m, 1H), 6.94 (s, 1H), 2.89 (d, *J* = 11.1 Hz, 2H), 2.70 (t, *J* = 7.8 Hz, 2H), 2.43 (s, 3H), 2.33 – 2.29 (m, 1H), 2.06 – 1.95 (m, 3H), 1.79 (d, *J* = 12.4 Hz, 2H), 1.53 – 1.38 (m, 4H). ^{13}C NMR (75 MHz, DMSO-d_6) δ 166.7, 153.8, 141.0, 139.6, 139.0, 134.9, 134.7, 129.8, 129.1, 128.7, 127.7, 126.2, 125.3, 125.2, 121.6, 60.1, 52.3, 48.8, 33.4, 32.1, 31.6, 29.5, 22.5. ESI-MS *m/z* 486 [*M* + Na]$^+$. HRMS(ESI) *m/z* [*M* + H]+ calcd for [$C_{26}H_{30}N_3O_3S$]$^+$ 464.2002, found 464.1990.

*4.1.40. 3-(3-Carbamoyl-5-methylthiophen-2-yl)phenylmethyl(1-phenethylpiperidin-4-yl)carbamate (**4j**)*

The title compound was prepared according to the procedure described for **31a**, starting from **5b** (40.0 mg, 0.17 mmol), 4-nitrophenyl chloroformate (51.0 mg, 0.25 mmol), TEA (71 µL, 0.51 mmol) and amine **6e** (54.5 mg, 0.25 mmol) in dry DCM (10.0 mL). The crude was purified by column chromatography on silica gel (EtOAc/MeOH from 50:1 to 20:1) to afford the title compound as an amorphous white solid (48.6 mg, 60% yield). ^{1}H NMR (300 MHz, CD_3OD) δ 7.44 – 7.32 (m, 2H), 7.31 – 7.14 (m, 6H), 7.13 – 7.07 (m, 1H), 6.99 – 6.95 (m, 1H), 4.18 – 3.94 (m, 1H), 3.16 (d, *J* = 11.5 Hz, 2H), 3.04 – 2.89 (m, 3H), 2.82 (dd, *J* = 10.6, 5.7 Hz, 2H), 2.68 – 2.60 (m, 2H), 2.48 – 2.45 (m, 3H), 2.28 – 2.13 (m, 2H), 2.02 – 1.71 (m, 4H). ^{13}C NMR (75 MHz, CD_3OD) δ 168.6, 154.9, 151.4, 141.1, 139.7, 139.6, 134.5, 132.7, 129.1, 128.2, 128.1, 126.6, 126.5, 125.8, 125.7, 121.9, 121.3, 59.9, 52.5, 32.8, 28.2, 13.5. ESI-MS *m/z* 500 [*M* + Na]$^+$.

*4.1.41. 3-(3-Carbamoyl-5-methylthiophen-2-yl)phenyl-4-(3-phenylpropyl)piperazine-1-carboxylate (**4k**)*

The title compound was prepared according to the procedure described for **31a**, starting from **5b** (10.0 mg, 0.04 mmol), 4-nitrophenyl chloroformate (12.0 mg, 0.06 mmol), TEA (20 μL, 0.15 mmol) amine **6f** (12.0 mg, 0.06 mmol) in dry DCM (3.0 mL). The crude was purified by column chromatography on silica gel (EtOAc/MeOH from 100:1 to 80:1) to afford the title compound as an amorphous yellow solid (14.2 mg, 77% yield) ^{1}H NMR (300 MHz, $CDCl_3$) 7.40 (t, *J* = 7.8 Hz, 1H), 7.36 – 7.21 (m, 5H), 7.24 – 7.12 (m, 3H), 7.12 (t, *J* = 2.3 Hz, 1H), 5.57 – 5.47 (brs, 2H), 3.66 (d, *J* = 30.5 Hz, 4H), 2.67 (t, *J* = 7.6 Hz, 2H), 2.59 – 2.46 (m, 6H), 2.46 (s, 3H), 1.97 – 1.78 (m, 2H).^{13}C NMR (75 MHz, $CDCl_3$) δ 166.8, 153.2, 151.4, 141.7,141.4, 139.3, 134.1, 132.4, 129.7, 128.4, 127.7, 126.9, 125.9, 123.1, 122.2, 57.7, 52.7, 52.6, 44.7, 43.7, 33.5, 29.7, 28.1. ESI-MS *m/z* 486 [*M* + Na]$^+$. HRMS(ESI) *m/z* [*M* + H]$^+$ calcd for $[C_{26}H_{30}N_3O_3S]^+$ 464.2002, found 464.1996, [*M* + Na]$^+$; calcd for $[C_{26}H_{29}N_3O_3NaS]^+$ 486.1822, found 486.1815.

*4.1.42. 3-(3-Carbamoyl-1H-pyrrol-1-yl)phenyl (1-phenethylpiperidin-4-yl)carbamate (**4l**)*

The title compound was prepared according to the procedure described for compound **31a**, starting from **5c** (40.0 mg, 0.20 mmol), 4-nitrophenyl chloroformate (60.0 mg, 0.30 mmol), TEA (83 μL, 0.60 mmol) and amine **6b** (61.0 mg, 0.30 mmol) in dry DCM (14.0 mL). The crude was purified by column chromatography on silica gel (EtOAc/MeOH from 20:1 to 10:1) to afford the title compound as an amorphous white solid (14.7 mg, 17% yield). ^{1}H NMR (300 MHz, DMSO-d_6) δ 7.97 – 7.83 (m, 1H), 7.52 – 7.34 (m, 5H), 7.32 – 7.11 (m, 4H), 7.08 – 6.97 (m, 1H), 6.96 – 6.81 (m, 2H), 6.64 (s, 1H), 3.49 (s, 1H), 2.91 (d, *J* = 11.0 Hz, 2H), 2.71 (t, *J* = 7.8 Hz, 2H), 2.56 – 2.50 (m, 2H), 2.14 – 1.97 (m, 3H), 1.84 – 1.72 (m, 2H), 1.56 – 1.38 (m, 2H). ^{13}C NMR (75 MHz, DMSO-d_6) δ 165.5, 153.7, 152.5, 140.9, 140.5, 130.9, 129.1, 128.7, 126.3, 122.7, 121.8, 120.4, 119.9, 116.4, 113.8, 110.9, 60.1, 52.3, 48.8, 33.4, 32.0, 31.2. ESI-MS *m/z* 433 [*M* +H]$^+$, 456 [*M* + Na]$^+$. HRMS(ESI) *m/z* [M + H]$^+$ calcd for $[C_{25}H_{29}N_4O_3]^+$ 433.2234, found 433.2216.

*4.1.43. 3-(3-Carbamoyl-1H-pyrrol-1-yl)phenylmethyl-1-phenethylpiperidin-4-yl)carboxylate (**4m**)*

The title compound was prepared according to the procedure described for **31a**, starting from **5c** (20.0 mg, 0.10 mmol), 4-nitrophenyl chloroformate (30.0 mg, 0.15 mmol), TEA (41 μL, 0.30 mmol) and amine **6e** (33.0 mg, 0.15 mmol) in dry DCM (6.0 mL). The crude was purified by column chromatography on silica gel (EtOAc/MeOH from 50:1 to 20:1) to afford the title compound as an amorphous white solid (13.8 mg, 31% yield). ^{1}H NMR (300 MHz, CD_3OD) δ 7.81 (s, 1H), 7.49 (t, *J* = 8.1 Hz, 1H), 7.42 – 7.31 (m, 3H), 7.30 – 7.14 (m, 5H), 7.12 – 7.06 (m, 1H), 6.73 (s, 1H), 4.21 – 3.98 (m, 1H), 3.19 (d, *J* = 11.5 Hz, 2H), 3.03 (s, 3H), 2.89 – 2.76 (m, 2H), 2.73 – 2.59 (m, 2H), 2.24 (d, *J* = 12.3 Hz, 2H), 2.05 – 1.71 (m, 4H). ^{13}C NMR (75 MHz, CD_3OD) δ 172.2, 158.5, 156.31, 144.6, 143.7, 134.2, 132.2, 132.1, 129.8, 126.0, 124.8, 124.2, 123.6, 120.9, 118.0, 114.0, 63.7, 56.4, 36.6, 32.5, 32.2, 31.8. ESI-MS *m*/*z* 469 $[M + Na]^+$

*4.1.44. 3-(3-Carbamoyl-1H-pyrrol-1-yl)phenyl 4-(3-phenylpropyl)piperazine-1-carboxylate (**4n**)*

The title compound was prepared according to the procedure described for **31a**, starting from **5c** (10.0 mg, 0.05 mmol), 4-nitrophenyl chloroformate (15.0 mg, 0.075 mmol), TEA (20 μL, 0.15 mmol) and amine **6f** (15.0 mg, 0.075 mmol) in dry DCM (6.0 mL). The crude was purified by column chromatography on silica gel (EtOAc/MeOH 30:1) to afford the title compound as an amorphous yellow solid (10.8 mg, 50% yield). ^{1}HNMR (300 MHz, $CDCl_3$) δ 7.67 (d, *J* = 2.0 Hz, 1H), 7.45 (t, *J* = 8.1 Hz, 1H), 7.37 – 7.26 (m, 4H), 7.27 – 7.18 (m, 3H), 7.11 (dd, *J* = 8.1, 2.2 Hz, 1H), 7.06 (s, 1H), 6.58 (s, 1H), 5.82 – 5.52 (brs, 2H), 3.67 (dd, *J* = 28.5, 6.1 Hz, 4H), 2.70 (t, *J* = 7.7 Hz, 2H), 2.58 – 2.50 (m, 4H), 2.46 (t, *J* = 7.5 Hz, 2H), 1.88 (p, *J* = 7.5 Hz, 2H).^{13}CNMR (75 MHz, $CDCl_3$) δ 166.2, 153.1, 152.3, 142.0, 140.6, 130.3, 128.4, 128.3, 125.8, 122.56, 120.8, 120.5, 120.0, 117.5, 114.8, 109.6, 57.8, 52.9, 52.7, 44.6, 44.1, 33.5, 28.4.ESI-MS *m*/*z* 433 $[M + H]^+$. HRMS(ESI) *m/z* $[M + H]^+$ calcd for $[C_{25}H_{29}N_4O_3]^+$ 433.2234, found 433.2221.

*4.1.45. 3-(4-Carbamoyl-1H-1,2,3-triazol-1-yl)phenyl (6-phenylhexyl)carbamate (**4o**)*

The title compound was prepared according to the procedure described for **31a**, starting from **5d** (20.0 mg, 0.10 mmol), 4-nitrophenyl chloroformate (30.0 mg, 0.15 mmol), TEA (41 μL, 0.30

mmol) amine **6d** (26.0 mg, 0.15 mmol) in dry DCM (7.0 mL). The crude was purified by column chromatography on silica gel (DCM/MeOH 100:1) to afford the title compound as a white solid (17.0 mg, 23% yield). ^{1}H NMR (300 MHz, DMSO-d_6) δ 9.27 (s, 1H), 8.02 (s, 1H), 7.91 (t, J = 5.6 Hz, 1H), 7.86 – 7.71 (m, 2H), 7.66 – 7.53 (m, 2H), 7.41 – 7.08 (m, 5H), 4.41 (t, J = 5.2 Hz, 1H), 3.05 (q, J = 6.7 Hz, 2H), 2.62 – 2.51 (m, 2H), 1.67 – 1.38 (m, 4H), 1.39 – 1.25 (m, 4H). ^{13}C NMR (75 MHz, DMSO-d_6) δ 163.6, 161.6, 154.3, 152.3, 144.3, 142.7, 137.3, 131.1, 128.8, 128.7 (2C), 128.2, 126.0, 122.9, 35.5, 31.4, 29.5, 28.8, 26.5. ESI-MS *m/z* 408 $[M + H]^+$. HRMS(ESI) *m/z* $[M + H]^+$ calcd for $[C_{22}H_{26}N_5O_3]^+$ 408.2030, found 408.2024, $[M + Na]^+$ calcd for $[C_{22}H_{25}N_5NaO_3]^+$ 430.1850 found 430.1843.

*4.1.46. 3-(4-Carbamoyl-1H-1,2,3-triazol-1-yl)phenyl 4-(3-phenylpropyl)piperazine-1-carboxylate (**4p**)*

The title compound was prepared according to the procedure described for **31a**, starting from **5d** (20.0 mg, 0.10 mmol), 4-nitrophenyl chloroformate (30.0 mg, 0.30 mmol), TEA (41 µL, 0.15 mmol) and a solution of the amine **6f** (26.0 mg, 0.15 mmol) in dry DCM (12.0 mL). The crude was purified by column chromatography on silica gel (DCM/MeOH from 70:1 to 10:1) to afford the title compound as an amorphous white solid (14.0 mg, 38% yield). ^{1}H NMR (300 MHz, DMSO-d_6) δ 9.25 (s, 1H), 8.06 – 7.95 (m, 2H), 7.84 – 7.75 (m, 2H), 7.65 – 7.52 (m, 2H), 7.34 – 7.08 (m, 5H), 3.63 – 3.36 (m, 4H), 2.58 (t, J = 7.7 Hz, 2H), 2.44 – 2.35 (m, 4H), 2.30 (t, J = 7.2 Hz, 2H), 1.72 (p, J = 7.6 Hz, 2H). ^{13}C NMR (75 MHz, DMSO-d_6) δ 161.6, 152.8, 152.4, 144.7, 142.4, 137.3, 131.1, 128.8, 128.7, 126.1, 125.4, 123.0, 117.4, 114.7, 57.5, 52.8, 44.6, 44.2, 33.3, 28.5. ESI-MS *m/z* 408 $[M + H]^+$. HRMS(ESI) *m/z* $[M + H]^+$ calcd for $[C_{23}H_{27}N_6O_3]^+$ 435.2139, found 435.2126.

*4.1.47. 5-Methyl-2-(3-(((6-phenylhexyl)carbamoyl)oxy)phenyl)furan-3-carboxylic acid (**4q**)*

The title compound was obtained according to the procedure described for compound **6c**, starting from **32** (21.0 mg, 0.04 mmol) in methanol (30.0 mL). The crude was purified by column chromatography on silica gel (PE/EtOAc 2:1 to 1:1) to afford the title compound as a brown solid (5.17 mg, 13% yield). ^{1}H NMR (300 MHz, $CDCl_3$) δ 7.88 – 7.79 (m, 1H), 7.79 – 7.72 (m, 1H), 7.39

(t, *J* = 8.0 Hz, 1H), 7.33 – 7.21 (m, 3H), 7.22 – 7.10 (m, 3H), 6.46 (s, 1H), 5.14 – 5.05 (brs, 1H), 3.25 (q, *J* = 6.7 Hz, 2H), 2.60 (t, *J* = 7.7 Hz, 2H), 2.34 (s, 3H), 1.70 – 1.50 (m, 4H), 1.37– 1.20 (m, 4H). ^{13}C NMR (75 MHz, $CDCl_3$) δ 167.8, 156.1, 154.4, 151.6, 150.8, 142.6, 130.9, 128.9, 128.4, 128.7, 125.6, 125.2, 122.5, 121.4, 113.8, 109.2, 41.2, 35.8, 31.3, 29.7, 28.9, 26.6, 13.3. ESI-MS *m/z* 422[M + H]$^+$. HRMS(ESI) *m/z* [M + Na]$^+$; calcd for $[C_{25}H_{27}NNaO_5]^+$ 444.1781, found 444.1774

*4.1.48. 5-Methyl-2-(3-((4-(3-phenylpropyl)piperazine-1-carbonyl)oxy)phenyl)furan-3-carboxylic acid (**4r**)*

The title compound was obtained according to the procedure described for compound **6c**, starting from **33** (21.0 mg, 0.04 mmol) in methanol (30.0 mL). The crude was purified by column chromatography on silica gel (DCM/MeOH from 60:1 to 40:1) to afford the title compound as a brown solid (15.3 mg, 39%yield).^{1}H NMR (300 MHz, $CDCl_3$) δ 9.39 – 8.33 (brs, 1H), 7.82 (s, 1H), 7.73 – 7.65 (m, 1H), 7.37 (t, *J* = 8.0 Hz, 1H), 7.31 – 7.21 (m, 2H), 7.20 – 7.04 (m, 4H), 6.44 (t, *J* = 1.0 Hz, 1H), 3.95 – 3.58 (m, 4H), 2.82 – 2.68 (m, 4H), 2.66 – 2.54 (m, 4H), 2.33 (s, 3H), 1.97 – 1.85 (m, 2H). ^{13}C NMR (75 MHz, $CDCl_3$) δ 162.2, 148.5, 148.0, 146.0, 145.4, 135.7, 126.6, 123.7, 123.3, 123.2, 123.1, 120.9, 119.6, 116.8, 116.5, 111.7, 104.4, 51.9, 46.6, 46.4, 37.8, 37.2, 28.1, 21.1. ESI-MS *m/z* 449 [*M* + H]$^+$, 472 [*M* + Na]$^+$. HRMS(ESI) *m/z* [*M* + H]$^+$ calcd for $[C_{26}H_{29}N_2O_5]^+$ 449.2071, found 449.2062.

*4.1.49. 3-(2H-Tetrazol-5-yl)phenyl (6-phenylhexyl)carbamate (**4s**)*

The title compound was prepared according to the procedure described for **31a**, starting from **5e** (15.0 mg, 0.10 mmol), 4-nitrophenyl chloroformate (28.0 mg, 0.15 mmol), TEA (41 µL, 0.27 mmol) and amine **6d** (26.0 mg, 0.15 mmol) in dry DCM (3.0 mL). The crude was purified by column chromatography on silica gel (DCM/MeOH/formic acid 30:1:0.1) to afford the title compound as a white solid (yield 17.3 mg, 52%). ^{1}H NMR (300 MHz, CD_3OD) δ 7.91 – 7.82 (m, 1H), 7.80 – 7.77 (m, 1H), 7.57 (t, *J* = 8.0 Hz, 1H), 7.36-7.31 (m, 1H), 7.26 – 7.07 (m, 5H), 3.24 – 3.13 (m, 2H), 2.60 (t, *J* = 8.5, 6.8 Hz, 2H), 1.70 – 1.51 (m, 4H), 1.47 – 1.32 (m, 4H). ^{13}C NMR (75 MHz, CD_3OD) δ 155.9, 155.2, 152.0, 142.5, 130.1, 128.0, 127.8, 125.6, 125.2, 124.5, 123.4, 120.2,

40.6, 35.4, 31.7, 29.6, 28.6, 26.3. ESI-MS *m/z* 366 $[M + H]^+$. HRMS(ESI) *m/z* $[M + H]^+$ calcd for $[C_{20}H_{24}N_5O_2]^+$ 366.1925, found 366.1921, $[M + Na]^+$ calcd for $[C_{20}H_{23}N_5NaO_2]^+$ 388.1744, found 388.1734.

*4.1.50 3-(2H-Tetrazol-5-yl)phenyl 4-(3-phenylpropyl)piperazine-1-carboxylate(**4t**)*

The title compound was prepared according to the procedure described for **31a**, starting from **5e** (25.0 mg, 0,154 mmol), 4-nitrophenyl chloroformate (47.0 mg, 0.23 mmol), TEA (65 µL, 0.46 mmol) and amine **6f** (47.0 mg 0.23 mmol) in dry DCM (10.0 mL). The crude was purified by column chromatography on silica gel (DCM/MeOH/formic acid 30:1:0.1) to afford the title compound as an amorphous white solid (yield 32.0 mg, 53%).^{1}H NMR (300 MHz, CD_3OD) δ 8.14 (s, 1H), 7.91 (dt, *J* = 7.8, 1.3 Hz, 1H), 7.82 (t, *J* = 1.9 Hz, 1H), 7.51 (t, *J* = 8.0 Hz, 1H), 7.32 – 7.09 (m, 5H), 4.04 – 3.66 (m, 4H), 3.40 – 3.23 (m, 4H), 3.18 – 3.01 (m, 2H), 2.68 (t, *J* = 7.4 Hz, 2H), 2.17 – 1.95 (m, 2H).^{13}C NMR (75 MHz, CD_3OD) δ 160.6, 154.4, 152.9, 141.4, 131.2, 130.5, 129.7, 129.4, 127.4, 125.1, 124.1, 121.2, 57.8, 52.7, 42.9, 42.3, 33.45, 26.91. ESI-MS *m/z* 393 $[M + H]^+$, 415 $[M + Na]^+$. HRMS(ESI) *m/z* $[M + H]^+$ calcd for $[C_{21}H_{25}N_6O_2]^+$ 393.2034, found 393.2028.

4.2. HPLC analysis

4.2.1 Solubility and chemical stability assay.

Solubility and chemical stability values, both calculated at pH = 3.0 and pH = 7.4 after 24h, were obtained in according with the procedures described in our previous work [22]. For each sample, the analysis was performed in triplicate and the solubility and chemical stability results reported, were determined from the average of the three values.

4.3 Computational Studies

4.3.1 Docking studies and MD simulations.

The X-ray structure of FAAH covalently bound to an alpha-ketoheterocycle inhibitor (PDB code: 3K84, chain A) was used to build the three-dimensional models of FAAH in complex with compounds **4e**, **4k**, **4n** and **4p** by docking. The protein structure was refined using the Protein Preparation Wizard tool available in Maestro [38–41] and setting a pH value of 9, at which the

enzyme shows its maximum activity [42]. Hydrogen atoms were added and the orientation of hydroxyl groups and conformations of asparagine and glutamine side chains were adjusted to maximize the number of hydrogen bonds. The catalytic Lys142 was modeled in its neutral form, in accordance with the catalytic mechanism of FAAH [27]. The obtained structure was submitted to a restrained minimization using the OPLS4 force field [43], in which only the hydrogen atoms were free to move. A second minimization was performed, in which also heavy atoms were free to move up to an RMSD value of 0.3 Å.

Michaelis-like complexes of FAAH and compounds **4e**, **4k**, **4n** and **4p** were generated by docking using Glide [44]. The structures of **4e**, **4k**, **4n** and **4p** were built in Maestro and prepared with the LigPrep tool [45] generating both the neutral and charge form for each compound. The docking grid was centered on the center of mass of the co-crystallized (9*Z*)-1-(5-pyridin-2-yl-1,3,4-oxadiazol-2-yl)octadec-9-en-1-one inhibitor. H-bond constraints between the oxyanion hole nitrogen of Ile238 and Gly239 and the carbonylic oxygen atom of **4e**, **4k**, **4n** and **4p** were added. Docking studies were performed using the standard precision (SP) mode and were forced to satisfy at least one of the two previously defined hydrogen bonds. Generated poses were ranked according to their Gscore values.

Michaelis complexes of FAAH-**4e** in its neutral and charge forms were also submitted to molecular dynamics (MD) simulations. The final systems were solvated using TIP3P water molecules in a simulation box 12 Å distant from the protein in every direction and neutralized by addition of 7 or 8 Cl^- ions for the neutral or charge form of **4e**, respectively. The Michaelis complexes were minimized and equilibrated for 5 ns under NVT and for 15 ns under NPT conditions, increasing the temperature up to 300 K and gradually reducing constraints on both the ligand and the protein. The production phase was carried out for 100 ns under NVT conditions using the Langevin thermostat. Harmonic restraints of 1 $kcal \cdot mol^{-1} \cdot Å^{-2}$ were applied on the backbone atoms. All bond lengths to hydrogen atoms were constrained using M-SHAKE. Short-range electrostatic interactions were cut off at 9 Å, whereas long-range electrostatic interactions were computed using the particle mesh Ewald method. A RESPA integrator was used with a time step of 2 fs, and long-range electrostatics

were computed every 6 fs. MD simulations were performed using the OPLS4 force field in Desmond 6.6 [28,46] both the Michaelis complexes two independent replicas of 100 ns were performed.

4.3.2 pK_a calculations

The pK_a constant for compounds **4e** and **4g** were calculated using Jaguar-pK_a workflow [30,47] which applies a set of equations based on DFT calculations and empirical correction to derive this thermodynamic constant. According to this approach an initial pK_a value ($pK_{a,raw}$) is obtained by applying equation 1:

$$pK_{a,raw} = \frac{\Delta G_a}{2.303 \times RT} \qquad (eq.\ 1)$$

Where ΔG_a is obtained from DFT calculations involving neutral and ionized forms of the compounds of interest by applying equation 2:

$$\Delta G_a = \Delta G_g - \Delta G_{sol}^{AH^+} + \Delta G_{sol}^{A} + \Delta G_{sol}^{H^+} \ (eq.\ 2)$$

where ΔG_g is the gas-phase deprotonation energy of the titratable compound, $\Delta G_{sol}^{AH^+}$ and $+\Delta G_{sol}^{A}$ are free energy of solvation of the protonated and deprotonated form, and $\Delta G_{sol}^{H^+}$ is the free-energy of solvation of the proton.

ΔG_g can be estimated by DFT gas-phase electronic energies of the protonated and deprotonated form of the molecule (E^{AH^+} and E^{A}), $\Delta G_{sol}^{AH^+}$ and ΔG_{sol}^{A} can be obtained by applying Poisson-Boltzmann equation protonated and deprotonated form of the molecule, while $\Delta G_{sol}^{H^+}$ is an experimentally deduced term.

$pK_{a,raw}$ is empirically corrected by equation 3, where a and b are functional-group specific parameters calculated through a calibration procedure, which allow to access a "nano" equilibrium constant, which represents the constant characterizing a protonation equilibrium between a single protonated conformation and a single deprotonated conformation.

$$pK_{a,nano} = a \times pK_{a,raw} + b \ (eq.\ 3)$$

Application of a Boltzmann-based correction scheme [30] accounting for the relative abundance of each conformation for the protonated or deprotonated form of the compound of interest returns a probability-weighted constant representing the final observable of this computational approach.

In our cases, phenyl 4-methylpiperazine-1-carboxylate and the phenyl 4-(methylamino)piperidine-1-carboxylate fragments of compound **4e** and **4g**, respectively, were build and submitted to DFT calculations with Jaguar. A conformational search for the protonated and deprotonated form of the two fragments was performed and the 5 most energetically favored conformations for each species were retained to apply the Boltzmann weighting scheme. Geometry optimization at B3LYP/6-31G* level for each conformer (protonated and deprotonated) was carried out, followed by single point energy calculations at B3LYP/cc-pVTZ level to access reliable gas-phase energies $E^{AH^+}$and E^A. Solvation energies ($\Delta G_{sol}^{AH^+}$and ΔG_{sol}^{A}) were computed applying the Poisson-Boltzmann equation on gas-phase optimized geometry. *a* and *b* empirical parameters applied here derive from a dataset of differently substituted tertiary amines [30].

4.4. Enzymatic studies

4.4.1. FAAH inhibition assay

The inhibition activity of the novel compounds towards *human* FAAH was tested with a fluorescence-based assay, following the manufacturer's instructions (Cayman Chemical, Ann Arbor, MI, USA). Briefly, compounds were pre-incubated at different concentrations with *human* FAAH for 30 min at 37 °C. The reaction was then initiated by the addition of 7-amino-4-methylcoumarin (AMC) arachidonoyl amide (final concentration 1 μM) as a substrate. After an incubation of 30 min at 37 °C, fluorescence due to the release of the AMC product was measured using an excitation wavelength of 355 nm and an emission wavelength of 465 nm in an EnSight Multimode plate reader (Perkin Elmer, MA, USA).

4.4.2. Evaluation of the mechanism of FAAH inhibition by rapid dilution assay.

Compounds **4e** and **4g** (10 and 100 nM) were incubated with a 50-fold concentrated solution of human FAAH enzyme for 30 min at 37 °C. Then, the enzyme inhibitor mixtures were diluted 50-

fold with assay buffer. After 30 min, aliquots of the mixtures were transferred into empty wells of the plate and the substrate was added. The enzyme activity was then measured according to the above-described standard procedure.

4.4.3. MAGL inhibition assay.

The inhibition activity of the novel compounds towards *human* MAGL was tested with a fluorescence-based assay, following the manufacturer's instructions (Biovision, Mountain View, CA, USA). Briefly, compounds were pre-incubated at different concentrations with *human* MAGL for 30 min at 37 °C. After the addition of the substrate 7-hydroxycoumarinyl arachidonate, the assay mixture was incubated for another 30 min at 37 °C and the resulting fluorescence was measured with an excitation at 360 nm and an emission at 460 nm using an EnSight Multimode plate reader (Perkin Elmer, MA, USA).

4.5. Cell-based assays

4.5.1. Cell culture and membrane preparation.

NIH3T3 and 1321N1 cells (Sigma-Aldrich) were maintained in DMEM (Invitrogen, Grand Island, NY, USA) supplemented with 10% FBS (Thermo Scientific, Waltham, MA, USA), *L*-glutamine (2 mM), penicillin (100 U/mL) and streptomycin (100 µg/mL) in a humidified atmosphere (5% CO_2) at 37 °C [48].

CHO cells transfected with human CBR_1 or CBR_2 (Perkin Elmer) were grown adherently and maintained in Ham's F12 containing 10% fetal bovine serum, penicillin (100 U/mL), streptomycin (100 µg/mL) and Geneticin (G418, 0.4 mg/mL) at 37 °C in 5% CO_2/95% air.

To obtain membranes, *h*CBR_1 and *h*CBR_2 CHO cells were washed with PBS and scraped off with ice-cold hypotonic buffer (5 mM Tris HCl, 2 mM EDTA, pH 7.4). The cell suspension was homogenized with a Polytron and then centrifuged for 30 min at 40,000 x g. The membrane pellet was suspended in 50 mM Tris HCl buffer (pH 7.4) containing 2.5 mM EDTA, 5 mM $MgCl_2$, 0.5 mg/mL BSA for CBR_1 or in 50 mM Tris HCl (pH 7.4), 1 mM EDTA, 5 mM $MgCl_2$, 0.5% BSA for CBR_2 [49].

4.5.2. [^{3}H]CP-55,940 competition binding assays

Competition binding experiments were carried out incubating 0.5 nM [^{3}H]-CP-55,940 (Perkin Elmer Life and Analytical Sciences, USA) and different concentrations of the tested compounds for 90 or 60 min at 30 °C with *h*CBR$_1$ or *h*CBR$_2$ CHO membranes (2 μg protein/100 μL), respectively. Non-specific binding was determined in the presence of 1 μM WIN 55,212-2 [49]. Bound and free radioactivity were separated by filtering the assay mixture through Whatman GF/C glass fiber filters using a Brandel cell harvester (Brandel Instruments, Unterföhring, Germany). The filter-bound radioactivity was counted using a Tri-Carb 2810TR liquid scintillation analyzer (Perkin Elmer).

4.5.3. NRU and MTT assays

NIH3T3 viability was evaluated by neutral red uptake (NRU) assay. Once at confluence, NIH3T3 fibroblasts were washed with 0.1 M PBS, separated with trypsin-EDTA solution, suspended in complete medium at a density of 1.5×10^4 cells/mL in each well of 24-well plates, and incubated at 37 °C in an atmosphere of 5% CO_2. After 24 h of culture, the test compounds solubilized in DMSO, were properly diluted in completed medium, and added to each well to test concentration values ranging from 0.6 to 180 μM. The experiments were repeated three times and all samples were set up in six replicates. Complete medium was used as negative control. After 24 of incubation, cell viability was evaluated by NRU assay using the procedure already reported [22].

4.5.4. MTT assay

1321N1 cell viability was determined by means of a 3-(4,5-dimethyl-2-thiazolyl)-2,5-diphenyl-2*H*-tetrazolium bromide (MTT) assay. For this purpose, cells were harvested from culture flasks by trypsinization and seeded into 96-well microculture plates at a cell density of $1x10^4$ cells/150 μL and incubated overnight in a humidified atmosphere (5% CO_2) at 37 °C. Cells were then exposed to different concentrations (10 nM – 30 μM) of selected novel compounds for 24 h.

After the incubation time, 15 μL of a 5 mg/mL MTT solution in PBS was added to each well and incubated 4 h in the dark. During this time MTT is converted to formazan by the mitochondrial

dehydrogenase in viable cells. At the end of the incubation, the formazan crystals are solubilized by adding 150 µL of an acidified isopropanolol solution. Optical densities at 570 nm were measured with the EnSight multimode plate reader (Perkin Elmer).

4.5.5. ROS production assay

1321N1 cells were seeded in 6-well plates at a density of 2.5×10^5 cells/2 mL and incubated overnight in a humidified atmosphere (5% CO_2) at 37 °C. Cells were pre-treated with selected novel compounds (1 nM – 1 µM) for 24 h before the exposure to 50 µM TBHP for 1 h at 37 °C. NAC (2 mM) was used as a reference antioxidant compound. At the end of the treatment period, 1 µM CellROX™ Green Reagent (Thermo-Fisher Scientific, Paisley, UK) was added to the cells followed by an incubation of 45 min at 37 °C. Immediately after cell detachment, data were acquired on an Attune NxT Flow Cytometer (Thermo-Fisher Scientific, Paisley, UK) equipped with a 488 nm laser for excitation and fluorescence emission was collected using a 530/30 BP filter. [48] 1321N1 cells were gated according to physical parameters and cell aggregates were removed from the analysis.

4.6. Ex vivo studies

4.6.1. Isolated Rat Heart Preparation and Perfusion

All experimental protocols, approved by the Animal Care and Ethics Committee of the University of Siena and Italian Department of Health (7DF-19.N.TBT) were carried out in compliance with the European Union Guidelines (D.L. 26/2014) for the Care and the Use of Laboratory Animals. Male Wistar rats (350 g, Charles River Italia, Calco, Italy), anaesthetized (i.p.) with a mixture of Zoletil® 100 (Virbac srl, Milano) and Rompun® (Bio 98, San Lazzaro, Bologna), containing heparin (5000 U/kg), were decapitated and exsanguinated. Specifically, spontaneously beating heart was mounted on a constant flow Langendorff apparatus for retrograde perfusion *via* the aorta as described elsewhere [50,51]. Hearts were allowed to equilibrate for at least 20 min before exposure to compound **4n**.

Heart contractility was measured as left ventricle pressure (LVP) by means of a deionized water-filled latex balloon, inserted into the left ventricle via the mitral valve and connected to a pressure

transducer (BLPR, WPI, Berlin, Germany). Alteration in coronary perfusion pressure (CPP), arising from changes in coronary vascular resistance, were recorded by a pressure transducer (BLPR, WPI, Berlin, Germany) placed in the inflow line [52].

A surface electrocardiogram (ECG) was recorded at a sampling rate of 1 kHz by means of two steel electrodes, one placed on the apex and the other on the left atrium of the heart. The ECG analysis included the following measurements: RR (cycle length), HR (frequency), PQ (atrioventricular conduction time), QRS (intraventricular conduction time), and QT (overall action potential duration) [53].

LVP, CPP, and ECG were recorded with a digital PowerLab data acquisition system (PowerLab 8/30; ADInstruments, Castle Hill, Australia) and analyzed by using Chart Pro for Windows software (PowerLab; ADInstruments, Castle Hill, Australia).

LVP was calculated by subtracting the left ventricular diastolic pressure from the left ventricular systolic pressure. As the QT interval is affected by heart rate changes (e.g., it shortens when heart rate increases), Bazett's formula normalized to average rat RR (QTc=QT/(RR/ f)1/2) [54] was routinely used to correct it, in order to avoid confounding effects. In our experiments, "f", the normalization factor according to the basal RR duration was 230 ms, as it was the average cardiac cycle length. Analysis of data was accomplished using GraphPad Prism version 5.04 (GraphPad Software, San Diego, USA). Statistical analyses and significance as measured by repeated measures ANOVA (followed by Dunnett's post-test) were obtained using GraphPad InStat version 3.06 (GraphPad Software, San Diego, USA). In all comparisons, $P < 0.05$ was considered significant.

Compound **4n** was dissolved in DMSO. Solvent failed to alter the response of the preparations (data not shown).

4.6.2. Ex vivo studies in hippocampal slices

All media and sera for OHSCs were purchased from Gibco (Milan, Italy). All animal experiments and handling and care were in accordance with the ARRIVE guidelines and the Guide for the Care and Use of Laboratory Animals. The experimental protocol was approved by the Animal Care and

Use Committee of "Federico II" University of Naples, Italy, and Ministry of Health, Italy (# 515/2019-PR). Female Wistar rats (14-day timed pregnant) were obtained from Charles River Laboratories (Italy) and maintained at a constant temperature (22 ± 1 °C) on a 12 h light/dark cycle (lights on at 7 AM) with food and water *ad libitum*. The pregnant dams were allowed to deliver their pups naturally; 7-9 days postpartum littermates were used for the preparation of organotypic explants. All efforts were made to minimize animal suffering and to reduce the number of animals used.

4.6.1. Rat hippocampal organotypic explants

Organotypic slice cultures were prepared as previously described [37,55,56]. Briefly, 400- μm-thick parasagittal slices were obtained from hippocampi of P7- to P9- day- old Wistar rat pups (Charles River Laboratories, Calco, Italy) using a McIlwain tissue chopper (Campden Instruments, Leicester, UK) and placed into ice- cold Hank's balanced salt solution (HBSS, Gibco, Italy) supplemented with 5 mg/mL glucose and 1.5% (v/v) Fungizone. Cultures were then transferred to a humidified semiporous membrane (30- mm Millicell tissue culture plate inserts of 0.4 mm pore size from Millipore, Italy) in six- well tissue culture plates (4 slices per membrane). Each well contained 1.2 mL of tissue culture medium consisting of 50% minimal essential medium (MEM, Gibco, Monza, Italy), 25% HBSS, 25% heat- inactivated horse serum, 6.5 mg/mL glucose, 1 mM glutamine, and 1.5% Fungizone. Cultures were maintained at a 37 °C and 5% CO_2- conditioned atmosphere. All experiments were performed on cultures kept *in vitro* for 10-12 days (DIV).

4.6.2. Lipopolysaccharide (LPS) plus interferon gamma (INF-γ) exposure and pharmacological treatments

Hippocampal explants were removed from normal serum-containing medium (NM) and exposed to a combined application of 10 μg/mL LPS plus 100 ng/mL INF–γ for 96 h in serum-free medium SFM (SFM, consisting of NM with serum replaced with MEM). This model triggers the release of massive proinflammatory and cytotoxic factors, and promotes an inflammatory neurodegeneration [57]. Appropriate concentration of each FAAH inhibitor: 0.3 nM -0.1 μM **4e**; 0.3 nM-0.1 μM **4g**; 3

nM-1 μM **4n**; 0.1-10 μM **4s**; or vehicle (DMSO ≤ 0.1%) were added to the medium at the beginning of the LPS+IFN-γ exposure and were kept in the culture medium during the entire duration of the experiment. Control culture explants, in the absence or in the presence of compounds, were kept in SFM.

Assessment of cell death and image analysis. Cell injury was assessed in explants by live incorporation of a marker of compromised membrane integrity, propidium iodide (PI, 5 μg/mL, Molecular Probes), that emits a bright red fluorescence when exposed to blue-green light. For densitometric measurements, the digital pictures were analyzed with the Image Pro-Plus software (Media Cybernetics), after freehand outlining of the CA1 neuronal layer, as previously described [37,55].

Statistical analysis. Statistical analysis was performed by using one-way ANOVA followed by Bonferroni post-hoc test as indicated in the legends of figures. Analysis was done using the software GraphPad Prism 5. Values represent the mean ± SEM of at least three independent experiments. Differences were considered statistically significant at * $p < 0.05$.

Acknowledgments

The authors wish to thank MIUR-PRIN n° 20175SA5JJ for financial support.

5. References

[1] H.C. Lu, K. Mackie, Review of the Endocannabinoid System, Biol. Psychiatry Cogn. Neurosci. Neuroimaging. 6 (2021) 607–615. https://doi.org/10.1016/j.bpsc.2020.07.016.

[2] E.A. Stein, S.A. Fuller, W.S. Edgemond, W.B. Campbell, Physiological and behavioural effects of the endogenous cannabinoid, arachidonylethanolamide (anandamide), in the rat, Br. J. Pharmacol. 119 (1996) 107–114. https://doi.org/10.1111/j.1476-5381.1996.tb15683.x.

[3] T. Sugiura, S. Kishimoto, S. Oka, M. Gokoh, Biochemistry, pharmacology and physiology of 2-arachidonoylglycerol, an endogenous cannabinoid receptor ligand, Prog. Lipid Res. 45 (2006) 405–446. https://doi.org/10.1016/j.plipres.2006.03.003.

[4] M.L. Yates, E.L. Barker, Inactivation and biotransformation of the endogenous cannabinoids

anandamide and 2-arachidonoylglycerol, Mol. Pharmacol. 76 (2009) 11–17. https://doi.org/10.1124/mol.109.055251.

[5] M.K. McKinney, B.F. Cravatt, Structure and Function of Fatty Acid Amide Hydrolase, Annu. Rev. Biochem. 74 (2005) 411–432. https://doi.org/10.1146/annurev.biochem.74.082803.133450.

[6] E. Dainese, S. Oddi, M. Simonetti, A. Sabatucci, C.B. Angelucci, A. Ballone, B. Dufrusine, F. Fezza, G. De Fabritiis, M. Maccarrone, The endocannabinoid hydrolase FAAH is an allosteric enzyme, Sci. Rep. 10 (2020) 1–11. https://doi.org/10.1038/s41598-020-59120-1.

[7] F. Aiello, G. Carullo, M. Badolato, A. Brizzi, TRPV1–FAAH–COX: The Couples Game in Pain Treatment, ChemMedChem. (2016) 1686–1694. https://doi.org/10.1002/cmdc.201600111.

[8] M. van der Stelt, W.B. Veldhuis, M. Maccarrone, P.R. Bär, K. Nicolay, G.A. Veldink, V. Di Marzo, J.F.G. Vliegenthart, Acute neuronal injury, excitotoxicity, and the endocannabinoid system, Mol. Neurobiol. 26 (2002) 317–346. https://doi.org/10.1385/MN:26:2-3:317.

[9] V. Di Marzo, D. Melck, T. Bisogno, L. De Petrocellis, Endocannabinoids: Endogenous cannabinoid receptor ligands with neuromodulatory action, Trends Neurosci. 21 (1998) 521–528. https://doi.org/10.1016/S0166-2236(98)01283-1.

[10] A. Papa, S. Pasquini, C. Contri, S. Gemma, G. Campiani, S. Butini, K. Varani, F. Vincenzi, Polypharmacological Approaches for CNS Diseases: Focus on Endocannabinoid Degradation Inhibition, Cells. 11 (2022) 471. https://doi.org/10.3390/cells11030471.

[11] P.L. McGeer, E.G. McGeer, Inflammation and neurodegeneration in Parkinson's disease, Park. Relat. Disord. 10 (2004) S3. https://doi.org/10.1016/j.parkreldis.2004.01.005.

[12] T. Behl, R. Makkar, A. Sehgal, S. Singh, N. Sharma, G. Zengin, S. Bungau, F.L. Andronie-Cioara, M.A. Munteanu, M.C. Brisc, D. Uivarosan, C. Brisc, Current trends in neurodegeneration: Cross talks between oxidative stress, cell death, and inflammation, Int. J. Mol. Sci. 22 (2021). https://doi.org/10.3390/ijms22147432.

[13] K.J. Barnham, C.L. Masters, A.I. Bush, Neurodegenerative diseases and oxidatives stress, Nat. Rev. Drug Discov. 3 (2004) 205–214. https://doi.org/10.1038/nrd1330.

[14] J. Knight, C. Caseldine, M. Boykoff, Forum review: Forum review, Geogr. J. 176 (2010) 267–269. https://doi.org/10.1111/j.1475-4959.2010.00371.x.

[15] E. Colombo, C. Farina, Astrocytes: Key Regulators of Neuroinflammation, Trends Immunol. 37 (2016) 608–620. https://doi.org/10.1016/j.it.2016.06.006.

[16] R.J. Henry, D.M. Kerr, D.P. Finn, M. Roche, FAAH-mediated modulation of TLR3-induced neuroinflammation in the rat hippocampus, J. Neuroimmunol. 276 (2014) 126–134. https://doi.org/10.1016/j.jneuroim.2014.09.002.

[17] N. Murphy, T.R. Cowley, C.W. Blau, C.N. Dempsey, J. Noonan, A. Gowran, R. Tanveer, W.M. Olango, D.P. Finn, V.A. Campbell, M.A. Lynch, The fatty acid amide hydrolase inhibitor URB597 exerts anti-inflammatory effects in hippocampus of aged rats and restores an age-related deficit in long-term potentiation, J. Neuroinflammation. 9 (2012) 1–11. https://doi.org/10.1186/1742-2094-9-79.

[18] S. Butini, M. Brindisi, S. Gemma, P. Minetti, W. Cabri, G. Gallo, S. Vincenti, E. Talamonti, F. Borsini, A. Caprioli, M.A. Stasi, S. Di Serio, S. Ros, G. Borrelli, S. Maramai, F. Fezza, G. Campiani, M. MacCarrone, Discovery of potent inhibitors of human and mouse fatty acid amide hydrolases, J. Med. Chem. 55 (2012) 6898–6915. https://doi.org/10.1021/jm300689c.

[19] S. Butini, S. Gemma, M. Brindisi, S. Maramai, P. Minetti, D. Celona, R. Napolitano, F. Borsini, W. Cabri, F. Fezza, L. Merlini, S. Dallavalle, G. Campiani, M. MacCarrone, Identification of a novel arylpiperazine scaffold for fatty acid amide hydrolase inhibition with improved drug disposition properties, Bioorganic Med. Chem. Lett. 23 (2013) 492–495. https://doi.org/10.1016/j.bmcl.2012.11.035.

[20] M. Brindisi, G. Borrelli, S. Brogi, A. Grillo, S. Maramai, M. Paolino, M. Benedusi, A. Pecorelli, G. Valacchi, L. Di Cesare Mannelli, C. Ghelardini, M. Allarà, A. Ligresti, P. Minetti, G. Campiani, V. di Marzo, S. Butini, S. Gemma, Development of Potent Inhibitors

of Fatty Acid Amide Hydrolase Useful for the Treatment of Neuropathic Pain, ChemMedChem. 13 (2018) 2090–2103. https://doi.org/10.1002/cmdc.201800397.

[21] A. Grillo, F. Fezza, G. Chemi, R. Colangeli, S. Brogi, D. Fazio, S. Federico, A. Papa, N. Relitti, R. Di Maio, G. Giorgi, S. Lamponi, M. Valoti, B. Gorelli, S. Saponara, M. Benedusi, A. Pecorelli, P. Minetti, G. Valacchi, S. Butini, G. Campiani, S. Gemma, M. Maccarrone, G. Di Giovanni, Selective Fatty Acid Amide Hydrolase Inhibitors as Potential Novel Antiepileptic Agents, ACS Chem. Neurosci. 12 (2021) 1716–1736. https://doi.org/10.1021/acschemneuro.1c00192.

[22] A. Grillo, G. Chemi, S. Brogi, M. Brindisi, N. Relitti, F. Fezza, D. Fazio, L. Castelletti, E. Perdona, A. Wong, S. Lamponi, A. Pecorelli, M. Benedusi, M. Fantacci, M. Valoti, G. Valacchi, F. Micheli, E. Novellino, G. Campiani, S. Butini, M. Maccarrone, S. Gemma, Development of novel multipotent compounds modulating endocannabinoid and dopaminergic systems, Eur. J. Med. Chem. 183 (2019) 111674. https://doi.org/10.1016/j.ejmech.2019.111674.

[23] J.R. Clapper, F. Vacondio, A.R. King, A. Duranti, A. Tontini, C. Silva, S. Sanchini, G. Tarzia, M. Mor, D. Piomelli, A second generation of carbamate-based fatty acid amide hydrolase inhibitors with improved activity in vivo., ChemMedChem. 4 (2009) 1505–1513. https://doi.org/10.1002/cmdc.200900210.

[24] C.M. Russo, A.A. Adhikari, D.R. Wallach, S. Fernandes, A.N. Balch, W.G. Kerr, J.D. Chisholm, Synthesis and initial evaluation of quinoline-based inhibitors of the SH2-containing inositol 5′-phosphatase (SHIP), Bioorg. Med. Chem. Lett. 25 (2015) 5344–5348. https://doi.org/https://doi.org/10.1016/j.bmcl.2015.09.034.

[25] T.A. Halgren, R.B. Murphy, R.A. Friesner, H.S. Beard, L.L. Frye, W.T. Pollard, J.L. Banks, Glide: A New Approach for Rapid, Accurate Docking and Scoring. 2. Enrichment Factors in Database Screening, J. Med. Chem. 47 (2004) 1750–1759. https://doi.org/10.1021/jm030644s.

[26] M. Mileni, S. Kamtekar, D.C. Wood, T.E. Benson, B.F. Cravatt, R.C. Stevens, Crystal Structure of Fatty Acid Amide Hydrolase Bound to the Carbamate Inhibitor URB597: Discovery of a Deacylating Water Molecule and Insight into Enzyme Inactivation, J. Mol. Biol. 400 (2010) 743–754. https://doi.org/https://doi.org/10.1016/j.jmb.2010.05.034.

[27] A. Lodola, M. Mor, S. Rivara, C. Christov, G. Tarzia, D. Piomelli, A.J. Mulholland, Identification of productive inhibitor binding orientation in fatty acid amide hydrolase (FAAH) by QM/MM mechanistic modelling, Chem. Commun. (2008) 214–216. https://doi.org/10.1039/B714136J.

[28] C. Lu, C. Wu, D. Ghoreishi, W. Chen, L. Wang, W. Damm, G.A. Ross, M.K. Dahlgren, E. Russell, C.D. Von Bargen, R. Abel, R.A. Friesner, E.D. Harder, OPLS4: Improving Force Field Accuracy on Challenging Regimes of Chemical Space, J. Chem. Theory Comput. 17 (2021) 4291–4300. https://doi.org/10.1021/acs.jctc.1c00302.

[29] A.D. Bochevarov, E. Harder, T.F. Hughes, J.R. Greenwood, D.A. Braden, D.M. Philipp, D. Rinaldo, M.D. Halls, J. Zhang, R.A. Friesner, Jaguar: A high-performance quantum chemistry software program with strengths in life and materials sciences, Int. J. Quantum Chem. 113 (2013) 2110–2142. https://doi.org/https://doi.org/10.1002/qua.24481.

[30] A.D. Bochevarov, M.A. Watson, J.R. Greenwood, D.M. Philipp, Multiconformation, Density Functional Theory-Based pKa Prediction in Application to Large, Flexible Organic Molecules with Diverse Functional Groups, J. Chem. Theory Comput. 12 (2016) 6001–6019. https://doi.org/10.1021/acs.jctc.6b00805.

[31] A. Vallone, S. D'Alessandro, S. Brogi, M. Brindisi, G. Chemi, G. Alfano, S. Lamponi, S.G. Lee, J.M. Jez, K.J.M. Koolen, K.J. Dechering, S. Saponara, F. Fusi, B. Gorelli, D. Taramelli, S. Parapini, R. Caldelari, G. Campiani, S. Gemma, S. Butini, Antimalarial agents against both sexual and asexual parasites stages: structure-activity relationships and biological studies of the Malaria Box compound 1-[5-(4-bromo-2-chlorophenyl)furan-2-yl]-N-[(piperidin-4-yl)methyl]methanamine (MMV019918) and analog, Eur. J. Med. Chem. 150

(2018) 698–718. https://doi.org/https://doi.org/10.1016/j.ejmech.2018.03.024.

[32] G. Campiani, C. Cavella, J.D. Osko, M. Brindisi, N. Relitti, S. Brogi, A.P. Saraswati, S. Federico, G. Chemi, S. Maramai, G. Carullo, B. Jaeger, A. Carleo, R. Benedetti, F. Sarno, S. Lamponi, P. Rottoli, E. Bargagli, C. Bertucci, D. Tedesco, D. Herp, J. Senger, G. Ruberti, F. Saccoccia, S. Saponara, B. Gorelli, M. Valoti, B. Kennedy, H. Sundaramurthi, S. Butini, M. Jung, K.M. Roach, L. Altucci, P. Bradding, D.W. Christianson, S. Gemma, A. Prasse, Harnessing the Role of HDAC6 in Idiopathic Pulmonary Fibrosis: Design, Synthesis, Structural Analysis, and Biological Evaluation of Potent Inhibitors, J. Med. Chem. 64 (2021) 9960–9988. https://doi.org/10.1021/acs.jmedchem.1c00184.

[33] R. Niranjan, Recent advances in the mechanisms of neuroinflammation and their roles in neurodegeneration, Neurochem. Int. 120 (2018) 13–20. https://doi.org/10.1016/j.neuint.2018.07.003.

[34] S.M. Borghi, V. Fattori, M.S.N. Hohmann, W.A. Verri, Contribution of Spinal Cord Oligodendrocytes to Neuroinflammatory Diseases and Pain, Curr. Med. Chem. 26 (2018) 5781–5810. https://doi.org/10.2174/0929867325666180522112441.

[35] E. Eljaschewitsch, A. Witting, C. Mawrin, T. Lee, P.M. Schmidt, S. Wolf, H. Hoertnagl, C.S. Raine, R. Schneider-Stock, R. Nitsch, O. Ullrich, The endocannabinoid anandamide protects neurons during CNS inflammation by induction of MKP-1 in microglial cells, Neuron. 49 (2006) 67–79. https://doi.org/10.1016/j.neuron.2005.11.027.

[36] N. Battista, M. Bari, A. Tarditi, C. Mariotti, A.C. Bachoud-Lévi, C. Zuccato, A. Finazzi-Agrò, S. Genitrini, M. Peschanski, S. Di Donato, E. Cattaneo, M. Maccarrone, Severe deficiency of the fatty acid amide hydrolase (FAAH) activity segregates with the Huntington's disease mutation in peripheral lymphocytes, Neurobiol. Dis. 27 (2007) 108–116. https://doi.org/10.1016/j.nbd.2007.04.012.

[37] F. Boscia, L. Annunziato, M. Taglialatela, Retigabine and flupirtine exert neuroprotective actions in organotypic hippocampal cultures., Neuropharmacology. 51 (2006) 283–294.

https://doi.org/10.1016/j.neuropharm.2006.03.024.

[38] Maestro, version 12.8, Schrödinger, LLC, New York, NY, 2021.

[39] Protein Preparation Wizard, Schrödinger, LLC, New York, NY, 2021.

[40] Impact, version 9.1, Schrödinger, LLC, New York, NY, 2021.

[41] Prime, version 6.4, Schrödinger, LLC, New York, NY, 2021.

[42] M.K. McKinney, B.F. Cravatt, Evidence for distinct roles in catalysis for residues of the serine-serine-lysine catalytic triad of fatty acid amide hydrolase, J. Biol. Chem. 278 (2003) 37393–37399. https://doi.org/10.1074/jbc.M303922200.

[43] T. Lu, Q. Chen, Shermo: A general code for calculating molecular thermochemistry properties, Comput. Theor. Chem. 1200 (2021) 113249. https://doi.org/https://doi.org/10.1016/j.comptc.2021.113249.

[44] Glide, version 9.1; Schrödinger, LLC: New York, 2021.

[45] Epik, version 5.6, Schrödinger, LLC, New York, NY, 2021.

[46] Desmond Molecular Dynamics System, D.E.Shaw Research, New York, NY, 2021.

[47] Jaguar, version 11.2, Schrödinger, LLC, New York, 2021.

[48] F. Vincenzi, S. Pasquini, S. Setti, S. Salati, R. Cadossi, P.A. Borea, K. Varani, Pulsed Electromagnetic Fields Stimulate HIF-1α-Independent VEGF Release in 1321N1 Human Astrocytes Protecting Neuron-Like SH-SY5Y Cells from Oxygen-Glucose Deprivation., Int. J. Mol. Sci. 21 (2020). https://doi.org/10.3390/ijms21218053.

[49] F. Vincenzi, M. Targa, C. Corciulo, M.A. Tabrizi, S. Merighi, S. Gessi, G. Saponaro, P.G. Baraldi, P.A. Borea, K. Varani, Antinociceptive effects of the selective CB2 agonist MT178 in inflammatory and chronic rodent pain models, Pain. 154 (2013) 864—873. https://doi.org/10.1016/j.pain.2013.02.007.

[50] F. Pessina, A. Gamberucci, J. Chen, B. Liu, P. Vangheluwe, B. Gorelli, S. Lorenzini, O. Spiga, A. Trezza, G. Sgaragli, S. Saponara, Negative chronotropism, positive inotropism and lusitropism of 3,5-di-t-butyl-4-hydroxyanisole (DTBHA) on rat heart preparations occur

through reduction of RyR2 Ca(2+) leak., Biochem. Pharmacol. 155 (2018) 434–443. https://doi.org/10.1016/j.bcp.2018.07.026.

[51] G. Carullo, S. Saponara, A. Ahmed, B. Gorelli, S. Mazzotta, A. Trezza, B. Gianibbi, G. Campiani, F. Fusi, F. Aiello, Novel Labdane Diterpenes-Based Synthetic Derivatives: Identification of a Bifunctional Vasodilator That Inhibits $Ca_V1.2$ and Stimulates $K_{Ca}1.1$ Channels, Mar. Drugs. 20 (2022) 515. https://doi.org/10.3390/md20080515.

[52] A. Ferrara, F. Fusi, B. Gorelli, G. Sgaragli, S. Saponara, Effects of freeze-dried red wine on cardiac function and ECG of the Langendorff-perfused rat heart., Can. J. Physiol. Pharmacol. 92 (2014) 171–174. https://doi.org/10.1139/cjpp-2013-0262.

[53] S. Saponara, A. Ferrara, B. Gorelli, A. Shah, M. Kawase, N. Motohashi, J. Molnar, G. Sgaragli, F. Fusi, 3,5-Dibenzoyl-4-(3-phenoxyphenyl)-1,4-dihydro-2,6-dimethylpyridine (DP7): A new multidrug resistance inhibitor devoid of effects on Langendorff-perfused rat heart, Eur. J. Pharmacol. 563 (2007) 160–163. https://doi.org/https://doi.org/10.1016/j.ejphar.2007.02.001.

[54] F. Fusi, M. Durante, B. Gorelli, M.G. Perrone, N.A. Colabufo, S. Saponara, MC225, a Novel Probe for P-glycoprotein PET Imaging at the Blood-brain Barrier: In Vitro Cardiovascular Safety Evaluation., J. Cardiovasc. Pharmacol. 70 (2017) 405–410. https://doi.org/10.1097/FJC.0000000000000536.

[55] F. Boscia, F. Ferraguti, F. Moroni, L. Annunziato, D.E. Pellegrini-Giampietro, mGlu1α receptors are co-expressed with CB1 receptors in a subset of interneurons in the CA1 region of organotypic hippocampal slice cultures and adult rat brain, Neuropharmacology. 55 (2008) 428–439. https://doi.org/https://doi.org/10.1016/j.neuropharm.2008.04.024.

[56] V. de Rosa, A. Secondo, A. Pannaccione, R. Ciccone, L. Formisano, N. Guida, R. Crispino, A. Fico, R. Polishchuk, A. D'Aniello, L. Annunziato, F. Boscia, D-Aspartate treatment attenuates myelin damage and stimulates myelin repair, EMBO Mol. Med. 11 (2019) e9278. https://doi.org/https://doi.org/10.15252/emmm.201809278.

[57] I.E. Papageorgiou, A. Lewen, L. V Galow, T. Cesetti, J. Scheffel, T. Regen, U.-K. Hanisch, O. Kann, TLR4-activated microglia require IFN-γ to induce severe neuronal dysfunction and death in situ, Proc. Natl. Acad. Sci. 113 (2016) 212–217. https://doi.org/10.1073/pnas.1513853113.